NTIA Report 96-326

A Study of the Electromagnetic Properties of Concrete Block Walls for Short Path Propagation Modeling

Christopher L. Holloway
Patrick L. Perini
Ronald R. Delyser
Kenneth C. Allen

report series

U.S. DEPARTMENT OF COMMERCE • National Telecommunications and Information Administration

NTIA Report 96-326

A Study of the Electromagnetic Properties of Concrete Block Walls for Short Path Propagation Modeling

Christopher L. Holloway
Patrick L. Perini
Ronald R. Delyser
Kenneth C. Allen

U.S. DEPARTMENT OF COMMERCE
Ronald H. Brown, Secretary

Larry Irving, Assistant Secretary
for Communications and Information

October 1995

CONTENTS

FIGURES

FIGURES (continued)

Page

A Study of the Electromagnetic Properties of Concrete Block Walls for Short Path Propagation Modeling

Christopher L. Holloway[1]
Patrick L. Perini[2]
Ronald R. DeLyser[3]
Kenneth C. Allen[1]

For short propagation paths, correctly representing reflections of electromagnetic energy from surfaces is critical for accurate signal level predictions. In this paper, the method of homogenization is used to determine the effective material properties of composite material commonly used in construction. The reflection and transmission coefficients for block walls and other types of materials calculated with these homogenized effective material properties are presented. The importance of accurately representing the reflections for signal level prediction models is also investigated. It is shown that a 5- to 10-dB error in received signal strength can occur if the composite walls are not handled appropriately. Such accurate predictions of signal propagation over short distance is applicable to microcellular personal communications services deployments in urban canyons as well as indoor wireless private branch exchanges and local area networks.

Key words: composite walls; concrete walls; propagation modeling; reflection coefficient; homogenization; effective material properties

1. INTRODUCTION

Much work on long path propagation through urban settings has been done in the past [1]-[10]. In most of this work, little attention is given to accurate representation of the reflection coefficient (Γ) of a wave striking building surfaces. In this paper the problem of electromagnetic wave interaction with composite walls is addressed. Some examples used here are concrete block walls and other composite structures depicted in Figures 1 and 2.

[1]The author is with Institute for Telecommunications Sciences, National Telecommunications and Information Administration, U.S. Department of Commerce, Boulder, 80303
[2]The author is with US West Advanced Technologies, Boulder, 80303
[3]The author is with Department of Electrical Engineering, University of Denver, Denver, 80208

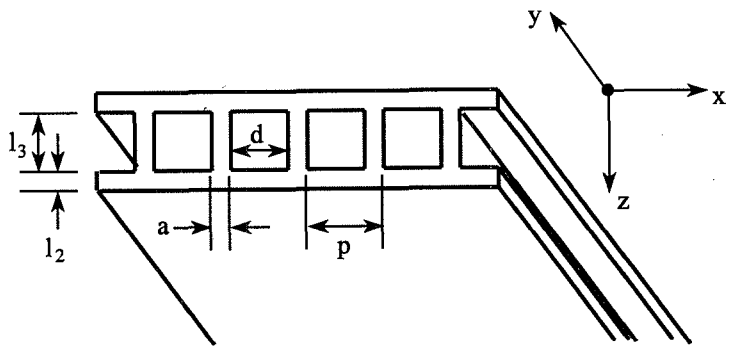

a)

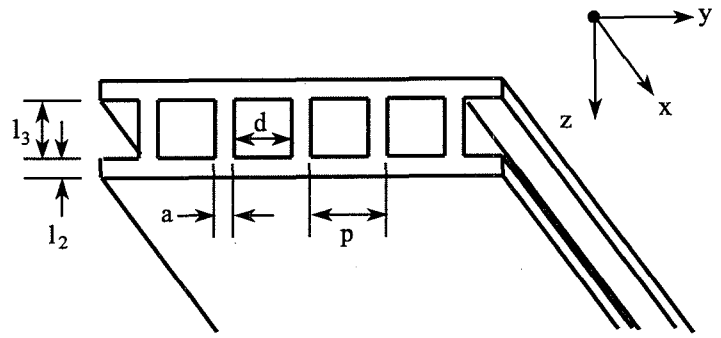

b)

Figure 1. a) Illustration of a concrete block wall with its slabs oriented along the $y - axis$, b) Illustration of a concrete wall with it slabs oriented along the $x - axis$.

In the majority of the published work the reflection coefficients of the buildings are obtained by assuming that either the building materials are perfect conductors or that the building walls are single solid slabs of material with some assumed properties. For the most part this may very well be justified for long path propagation in urban canyons.

In long path propagation, the transmitting and receiving antennas are set a relatively large distance apart. The dominant contribution to the total signal for an urban canyon setting is waves that make one to two bounces off the building, take a direct path, and make one bounce off the ground (see Figure 3). In this case the waves that bounce off of buildings are incident at an angle close to grazing, or 90^o. Even though the angular dependence of

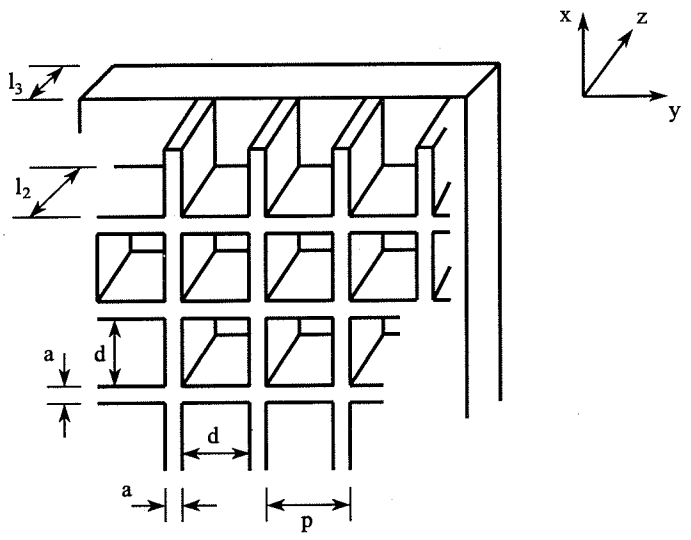

Figure 2. Illustration of a two-dimensional periodic block wall.

the reflection coefficient of a composite material can behave much differently than that of a perfect conductor or a single solid slab, this is not an important issue for long propagation paths. Therefore, regardless of the building's material, the actual reflection coefficient for large incident angles will approach that of a perfect conductor.

There is a growing need to predict signal levels for short propagation paths, in the range of 2-100 meters. Business campuses utilizing wireless private branch exchanges (PBXs) and wireless local area networks (LANs) to provide mobile voice and data communications, vehicular communications through urban canyons to nearby relays, and microcellular personal communications services (PCS) deployment in malls and airport are just a few examples. For short propagation paths like these, the accurate behavior of waves reflecting off walls can be very important.

Calculating the fields interaction (i.e. the reflection and transmission coefficient) of the composite structures similar to those shown in Figures 1 and 2 is a classic problem (see [11]-[27]). These techniques range from analytical techniques like Floquet analysis and mode matching to full numerical approaches like method of moments (MOM), finite element, and finite

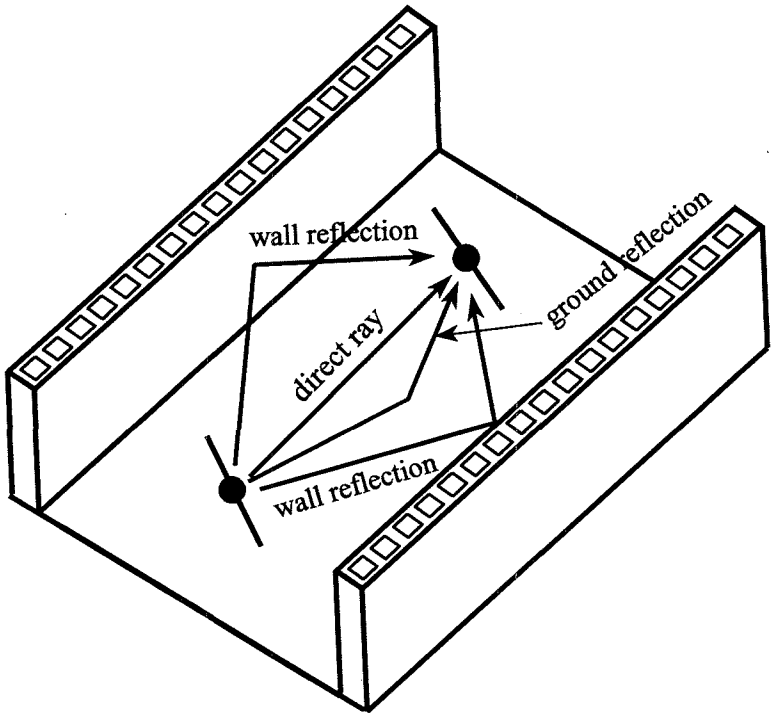

Figure 3. Illustration of the rays in the four-ray model.

difference methods. These techniques are capable of high accuracy, but are computationally intensive and hence do not lend themselves to ready use in signal prediction models. For short path signal prediction models (like ray tracing and other geometric optic models), efficient closed form expressions for calculating both the the reflection and transmission coefficients for composite structures are desired.

In this paper, we introduce expressions for the effective material properties for some commonly used composite building materials. These expressions for the effective material properties can be used to efficiently obtain the reflection and transmission coefficients for walls composed of composite materials. With these reflection and transmission properties we investigate the importance of accurately representing the interaction of the composite walls for the prediction of received signal strength (RSS) over short distances. The paper is organized as follows: following the introduction, Section 2 discusses the technique of homogenization, showing how the equivalent material properties for composite walls can be obtained. Ex-

pressions are then given for the effective material properties for both singly and doubly periodic structures. In Section 3 the equations needed for calculating the reflection and transmission coefficient for an obliquely incident plane wave (either perpendicular or parallel polarizations) are introduced. In Section 4 results from a singly periodic structure for different orientations and polarizations are presented. In Section 5 results for doubly periodic structures are presented. Also in Section 4 and 5, the importance of accurately representing the reflection properties of walls for signal level prediction models is investigated. Finally, in Section 6 a discussion on the validity of the expressions presented here is given.

2. EFFECTIVE MATERIAL PROPERTIES OBTAINED FROM HOMOGENIZATION

The problem at hand is to determine the reflection and/or transmission coefficient for a field incident onto the composite periodic structures illustrated in Figures 1 and 2. The concrete block wall in Figure 1 is equivalent to a five layer medium depicted in Figure 4. Layers 1 and 5 are free space, layers 2 and 4 have the material properties of the concrete, and layer 3 represents a one-dimensional periodic structure. The two-dimensional composite wall in Figure 2 is equivalent to a four-layer medium depicted in Figure 5. Layers 1 and 4 are free space, layer 3 has the material properties of the concrete, and layer 2 represents a two-dimensional periodic structure. In order to calculate the reflection and/or transmission coefficient for these composite structures the field's interaction with the periodic sections labeled as layer 3 (for the one-dimensional structure of Figure 4) and layer 2 (for the two-dimensional structure of Figure 5) must be determined.

Recently, a method for analyzing periodic structures known as homogenization has been used to solve problems of this type when the period of the structure is small compared to

the wavelength. Only a few of these published results are applicable to electromagnetic problems: [28] and [29] for a corrugated impedance surface, [30] and [31] for a wire grid and conducting strips, [32] for a rough perfectly and non-perfectly conducting rough surfaces, and [33]-[35] for analyzing pyramidal electromagnetic absorbers.

Even though the homogenization technique is based on the period of the structure being small compared to a wavelength, results given in [34] and [36]-[38] indicate that the homogenization models are accurate for periods at least as large as 1/2-1 free space wavelength and possibly even higher for lossy periodic structures. This is discussed in more detail in Section 6.

Homogenization is a technique utilized in the early 1970's, primarily by a group of French mathematicians (see [28] and [39]-[45]). This asymptotic technique is based on the method of multiple-scales associated with the microscopic and macroscopic field variations due to the periodic structure. In most situations, only the averaged (slowly varying) fields are of interest, and not the microstructure of the fields. Homogenization allows the separation of the average field from the microstructure. It is then possible to show that the averaged fields satisfy Maxwell's equations for some homogeneous media. The equivalent material properties of these homogeneous media are related to the properties of the composite structure.

With homogenization, the periodic layers of the composite structures (layer 3 in Figure 4 and layer 2 in Figure 5) can be replaced with a medium with an equivalent material property. Once the equivalent material property of the medium is determined, then the reflection and transmission coefficients of the composite structures can be efficiently obtained with either classical layered media approaches or by classical transmission line methods.

Homogenization uses asymptotic expansions and the concept of multiple-scales to expand the E and H fields in an asymptotic power series with both *slow* and *fast* variations. These slow and fast variations are associated with the microscopic and macroscopic field variations. With asymptotic power series of both the E and H fields, Maxwell's equations can be grouped

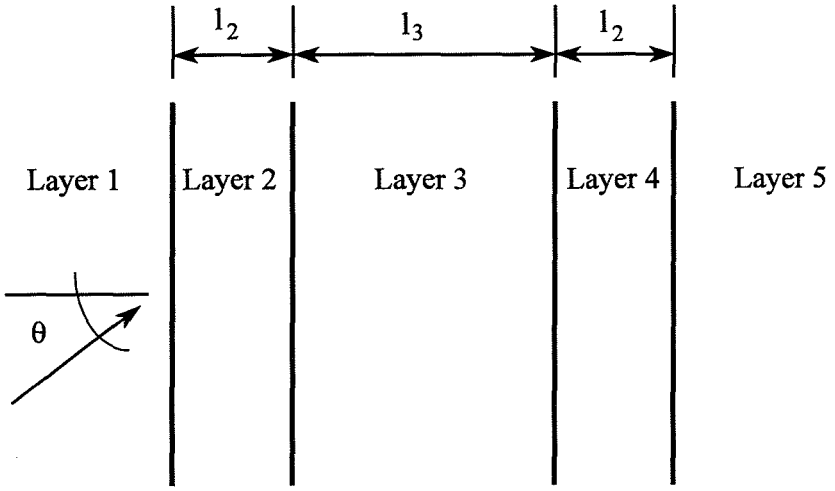

Figure 4. Equivalent layered media of a concrete block wall.

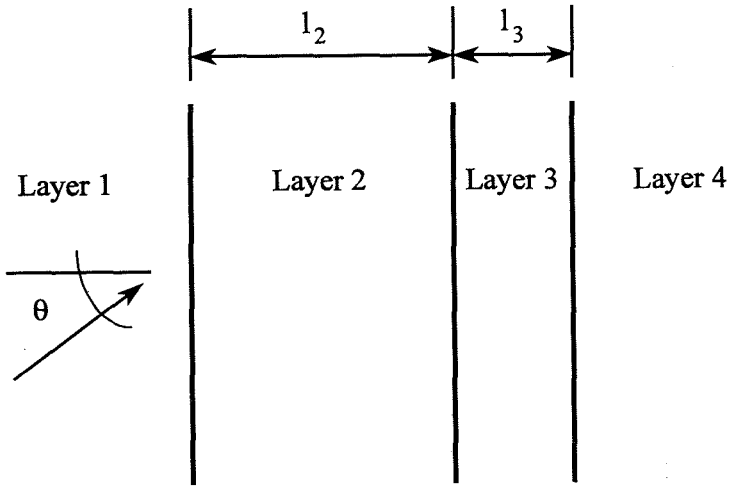

Figure 5. Equivalent layered media of a two-dimensional block wall.

in terms of different powers of the period (p) of the structure. The details of this procedure are found in [33].

Following this type of analysis, the zeroth order averaged fields $[(\bar{E}^o)_{\text{avg}}$ and $(\bar{H}^o)_{\text{avg}}]$ are related by the following:

$$\begin{aligned} \nabla \times (\bar{E}^o)_{\text{avg}} &= -j\omega \left[\mu^h\right] \cdot (\bar{H}^o)_{\text{avg}} \\ \nabla \times (\bar{H}^o)_{\text{avg}} &= -j\omega \left[\epsilon^h\right] \cdot (\bar{E}^o)_{\text{avg}} \ . \end{aligned} \tag{1}$$

This equation states that the average fields satisfy Maxwell's equations in an anisotropic homogeneous medium characterized by the tensors $\left[\epsilon^h\right]$ and $\left[\mu^h\right]$. These effective material properties are referred to as the homogenized permittivity $[\epsilon^h]$ and permeability $[\mu^h]$, and are defined by the following:

$$\begin{aligned} \left(\epsilon \bar{E}^o\right)_{\text{avg}} &\equiv \left[\epsilon^h\right] \cdot \left(\bar{E}^o\right)_{\text{avg}} \\ \left(\mu \bar{H}^o\right)_{\text{avg}} &\equiv \left[\mu^h\right] \cdot \left(\bar{H}^o\right)_{\text{avg}} \ . \end{aligned} \tag{2}$$

The average zero order fields $[(\bar{E}^o)_{\text{avg}}$ and $(\bar{H}^o)_{\text{avg}}]$ see the properties of the medium in terms of a single tensor quantity. The values of these tensors can be obtained from the solutions of the two-dimensional static source-free field problems that govern $\bar{E}^o$ and $\bar{H}^o$ (see [33]):

$$\begin{aligned} \nabla_\xi \times \bar{E}^o &= 0 \\ \nabla_\xi \times \bar{H}^o &= 0 \end{aligned} \tag{3}$$

and

$$\begin{aligned} \nabla_\xi \cdot (\epsilon \bar{E}^o) &= 0 \\ \nabla_\xi \cdot (\mu \bar{H}^o) &= 0 \end{aligned} \tag{4}$$

where ξ is the so-called *fast* variable and is defined as the following:

$$\xi = \frac{1}{p}(x\bar{a}_x + y\bar{a}_y) \tag{5}$$

where p is the period of the structure.

Now that it has been shown that the averaged field sees the periodic medium as an effective

anisotropic homogeneous region with tensor permittivity $[\epsilon^h]$ and $[\mu^h]$:

$$\begin{aligned} \left[\epsilon^h\right] &= \begin{bmatrix} \epsilon_x & 0 & 0 \\ 0 & \epsilon_y & 0 \\ 0 & 0 & \epsilon_x \end{bmatrix} \\ \left[\mu^h\right] &= \begin{bmatrix} \mu_x & 0 & 0 \\ 0 & \mu_y & 0 \\ 0 & 0 & \mu_x \end{bmatrix} , \end{aligned} \tag{6}$$

we now need to determine the effective material properties of this region. There has been a great deal of attention in the past towards determining the effective properties of composite regions. For a survey of this work see [46].

For the one-dimensional periodic structure, the effective properties of layer 3 (see Figure 4) is needed. If the period (p) of the slab structure shown in Figure 6 is small compared to a wavelength in either medium, and also small compared to the skin depth, then the effective properties are given by [33], [17] and [47]-[50] as:

$$\begin{aligned} \epsilon_x^{-1} &= (1-g)\epsilon_o^{-1} + g\epsilon_a^{-1} \\ \mu_x^{-1} &= (1-g)\mu_o^{-1} + g\mu_a^{-1} \\ \epsilon_y = \epsilon_z &= (1-g)\epsilon_o + g\epsilon_a \\ \mu_y = \mu_z &= (1-\acute{g})\mu_o + g\mu_a \end{aligned} \tag{7}$$

where $g = a/p$ (p and a are defined in Figure 1) is the relative volume of space occupied by the material, ϵ_a and μ_a are the complex parameters of the bulk material, and ϵ_o and μ_o are the free space values.

For the two-dimensional block wall shown Figure 7 (where $\epsilon_2 = \epsilon_o$ and $\epsilon_1 = \epsilon_a$), the longitudinal permittivity and permeability are known exactly ([46], [28] and [39]) as:

$$\begin{aligned} \epsilon_z &= (1-g)\epsilon_o + g\epsilon_a \\ \mu_z &= (1-g)\mu_o + g\mu_a \end{aligned} \tag{8}$$

where $g = a^2/p^2$ (a and p are defined in Figure 2) is the volume fraction of space occupied by the material, and ϵ_a and μ_a are the complex parameters of the bulk material.

For this type of symmetric two-dimensional periodic structure, $\epsilon_t = \epsilon_x = \epsilon_y$, and $\mu_t = \mu_x = \mu_y$. Reference [33] indicates that the transverse permittivity (ϵ_t) and permeability

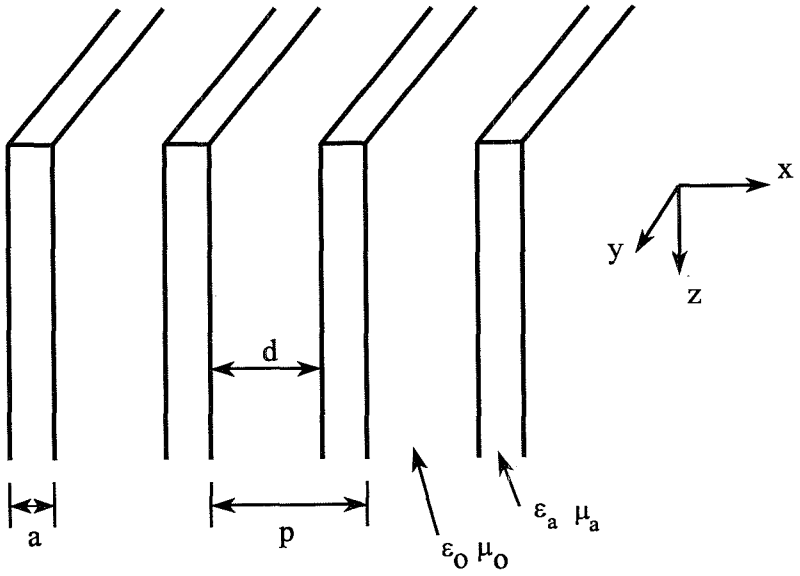

Figure 6. One-dimensional periodic structure.

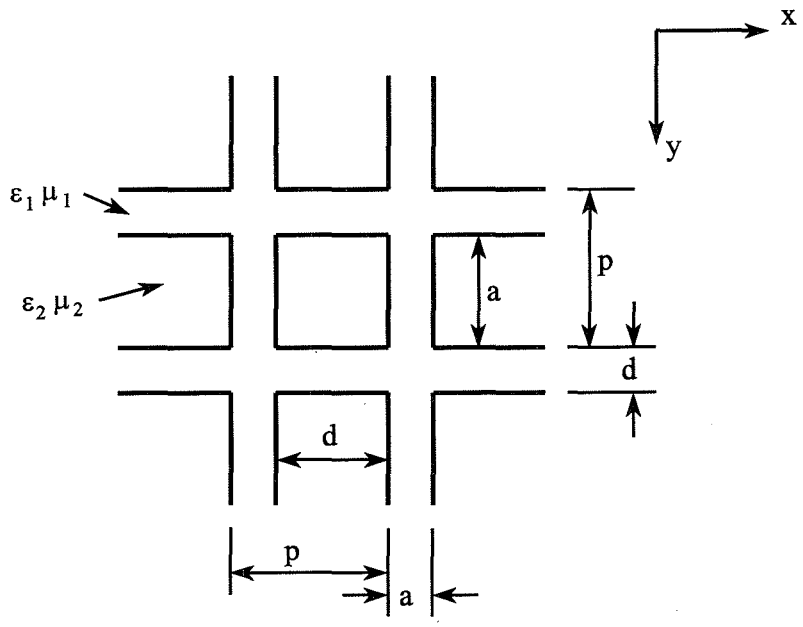

Figure 7. Two-dimensional periodic structure.

(μ_t) are not simple spatial averages as had often been assumed. There are no exact closed form expressions for the transverse material properties; however, upper and lower bounds for these properties can be found in [46].

Nakamura and Hirasawa [51] have done a numerical study of a similar periodic structure and they showed that the Hashin-Shtrikman upper bound given in [46] and [52] correlates very well to the effective material properties of this type of periodic structure. Thus, the transverse material properties can be approximated by the following:

$$\left.\begin{aligned} \epsilon_t &= \epsilon_a + \frac{1-g}{\frac{1}{\epsilon_a-\epsilon_o}+\frac{g}{2\epsilon_a}} \\ \mu_t &= \mu_a + \frac{1-g}{\frac{1}{\mu_a-\mu_o}+\frac{g}{2\mu_a}} \end{aligned}\right\} \tag{9}$$

where once again $g = a^2/p^2$ is the volume fraction of space occupied by the material.

In [33], a structure converse to the one shown in Figure 7, i.e., a dielectric surrounded by air (where $\epsilon_2 > \epsilon_1$), was analyzed. If the roles of the material properties in equation (9) are interchanged with Keller's scaling theorem [53] (such that $\epsilon_1 < \epsilon_2$), then the results given in equation (25) of [33] are obtained.

In general, the permittivity given in equations (7)-(9) is complex, resulting from the possibility that the material has a conductivity σ. For this scenario, the complex permittivity in these equations is expressed as:

$$\epsilon = \epsilon_r - j\frac{\sigma}{\epsilon_o\omega} \ . \tag{10}$$

3. OBLIQUELY INCIDENT PLANE WAVE

We want to investigate the problem of a plane wave incident onto the medium that behaves like a uniaxially anisotropic, but homogeneous, material. The periodic structures shown in

Figures 6 and 7 can be replaced with an equivalent layer (Figure 8). The material properties of this effective layer can be given by either equation (7) (for the one-dimensional periodic structure) or by equations (8) and (9) (for the two-dimensional periodic structure). If the plane of incidence is the xz-plane (Figure 8), then we can assume $\partial/\partial y \equiv 0$. Maxwell's equations can now be decoupled into two independent sets of equations; one set for the perpendicular polarization (referred to as E-polarization):

$$\begin{aligned} \frac{\partial H_x}{\partial z} - \frac{\partial H_z}{\partial x} &= j\omega\epsilon_y E_y \\ \frac{\partial E_y}{\partial x} &= -j\omega\mu_z H_z \\ \frac{\partial E_y}{\partial z} &= -j\omega\mu_x H_x \end{aligned} \tag{11}$$

and one set for the parallel polarization (referred to as H-polarization):

$$\begin{aligned} \frac{\partial E_x}{\partial z} - \frac{\partial E_z}{\partial x} &= j\omega\mu_y H_y \\ \frac{\partial H_y}{\partial x} &= -j\omega\epsilon_z E_z \\ \frac{\partial H_y}{\partial z} &= -j\omega\epsilon_x E_x \end{aligned} \tag{12}$$

with an assumed time factor of $e^{j\omega t}$.

The x-dependent factor of the fields is given by: $e^{-jk_o x \sin\theta}$, which means that the derivatives with respect to x can be replaced by:

$$\frac{\partial}{\partial x} \rightarrow -jk_o \sin\theta \ . \tag{13}$$

With this, the following general set of equations for the electromagnetic fields is obtained in which the z component is eliminated:

$$\begin{aligned} \frac{dE(z)}{dz} &= -j\omega\mu_{eff} H(z) \\ \frac{dH(z)}{dz} &= -j\omega\epsilon_{eff} E(z) \end{aligned} \tag{14}$$

where for the perpendicular polarization:

$$E(x) = E_y(z) \qquad H(z) = -H_x(z) \tag{15}$$

$$\begin{aligned} \epsilon_{eff} &= \epsilon_y - \frac{\mu_o \epsilon_o \sin^2\theta}{\mu_z} \\ \mu_{eff} &= \mu_x \end{aligned} \tag{16}$$

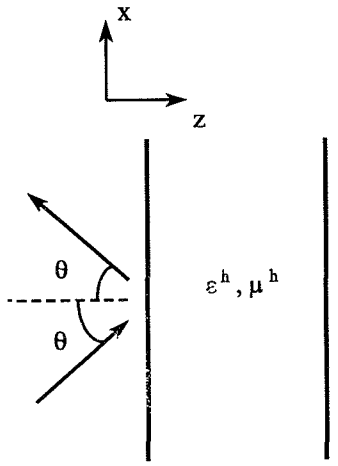

Figure 8. Equivalent anisotropic layer.

and for the parallel polarization:

$$E(x) = E_x(z) \qquad H(z) = H_y(z) \tag{17}$$

$$\begin{aligned} \epsilon_{eff} &= \epsilon_x \\ \mu_{eff} &= \mu_y - \frac{\mu_o \epsilon_o \sin^2\theta}{\epsilon_z} \ . \end{aligned} \tag{18}$$

With these expressions for the angular dependence on the effective material properties, we can now calculate reflection and transmission coefficients for composite structures.

4. REFLECTION FROM A CINDER BLOCK WALL

In this section, results for a one-dimensional periodic structure resembling a cinder block wall will be given (see Figures 1 and 4). Four block walls are analyzed: two different 14.5-cm (5.71-in) walls, one 7.2-cm (2.83-in) wall, and one 19.6-cm (7.72-in) wall. The dimensions of these different walls are shown in Table 1.

The 14.5-cm (5.71-in) block wall labelled block # 1 in Table 1 is represented as the layered structure shown in Figure 4, and has the following geometry: layers 1 and 5 are free space;

Table 1. Geometries of the concrete blocks

	Block # 1 [14.5-cm wall]	Block # 2 [14.5-cm wall]	Block # 3 [7.2-cm wall]	Block # 4 [19.6-cm wall]
l_2	2.25 cm	2.25 cm	1.7 cm	3.4 cm
l_3	10.0 cm	10.0 cm	3.8 cm	12.8 cm
a	2.6 cm	2.6 cm	2.8 cm	2.7 cm
d	14.3 cm	14.3 cm	9.5 cm	15.3 cm
ϵ_r	3.0	6.0	3.0	3.0
σ	$1.95 \cdot 10^{-3}$	$1.95 \cdot 10^{-3}$	$1.95 \cdot 10^{-3}$	$1.95 \cdot 10^{-3}$

layers 2 and 4 are a solid medium with $l_2 = 2.25\ cm$, $\mu = \mu_o$, $\epsilon_r = 3$ and $\sigma = 1.95 \cdot 10^{-3}$; and layer 3 is a medium with effective material properties given by equations (8) and (9) where $a = 2.6\ cm$, $d = 14.3\ cm$, $l_3 = 10.0\ cm$, $\epsilon_a = 3$ and $\sigma = 1.95 \cdot 10^{-3}$. Once the material properties of these layers are determined, the reflection coefficient can be obtained by using either classical layered media methods or classical transmission line methods. Figure 9 shows results for the reflectivity (defined as the magnitude squared of the reflection coefficient) of a block wall oriented both along the y-axis and x-axis (see Figure 1) for a perpendicularly polarized E field with a frequency of 900 MHz. Figure 10 shows results for a parallel polarization of the E field. These results were obtained using equations (16) and (18). Also shown in these figures are results for a solid layer of concrete ($\epsilon_r = 3$ and $\sigma = 1.95 \cdot 10^{-3}$) 14.5-cm thick.

From these figures it is apparent that the resonant behavior of the reflectivity cannot be achieved if a composite wall (block wall) is approximated by a solid layer. Correctly representing this resonant behavior is important for short path propagation. For large path propagation the reflection coefficient needed will correspond to angles approaching grazing (90^o), and from Figures 9 and 10 show that the reflection coefficient for the composite wall and the solid wall approach one another. This point is further illustrated in the following example.

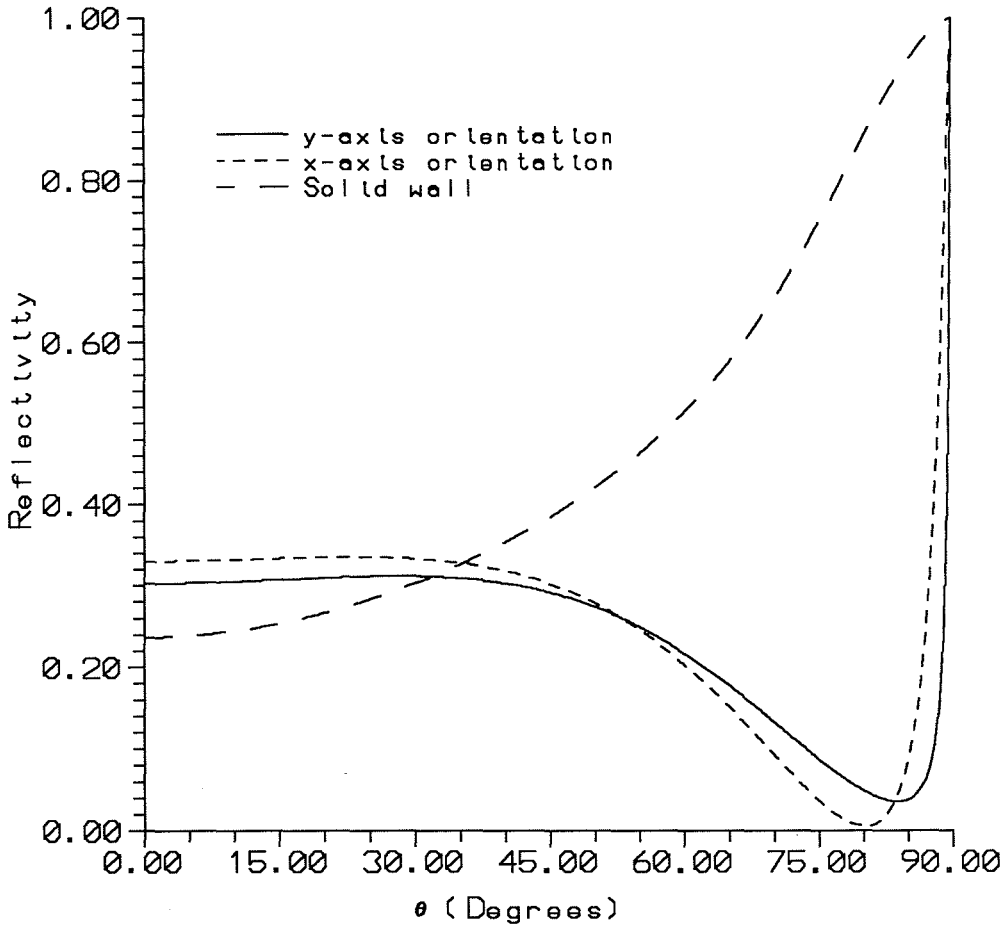

Figure 9. Reflectivity versus angle of incidence for a perpendicular polarized wave. These results are for block # 1 (see Table 1) with slabs oriented along both the $y-axis$ and $x-axis$ and with $f = 900$ MHz. The large dashed curve represents the results for a single layered slab of thickness equal to $2l_2 + l_3$, the solid curve represents the actual concrete block wall with the slabs oriented along the $y-axis$, and the small dashed curve represents the results for the actual concrete block wall with the slabs oriented along the $x-axis$.

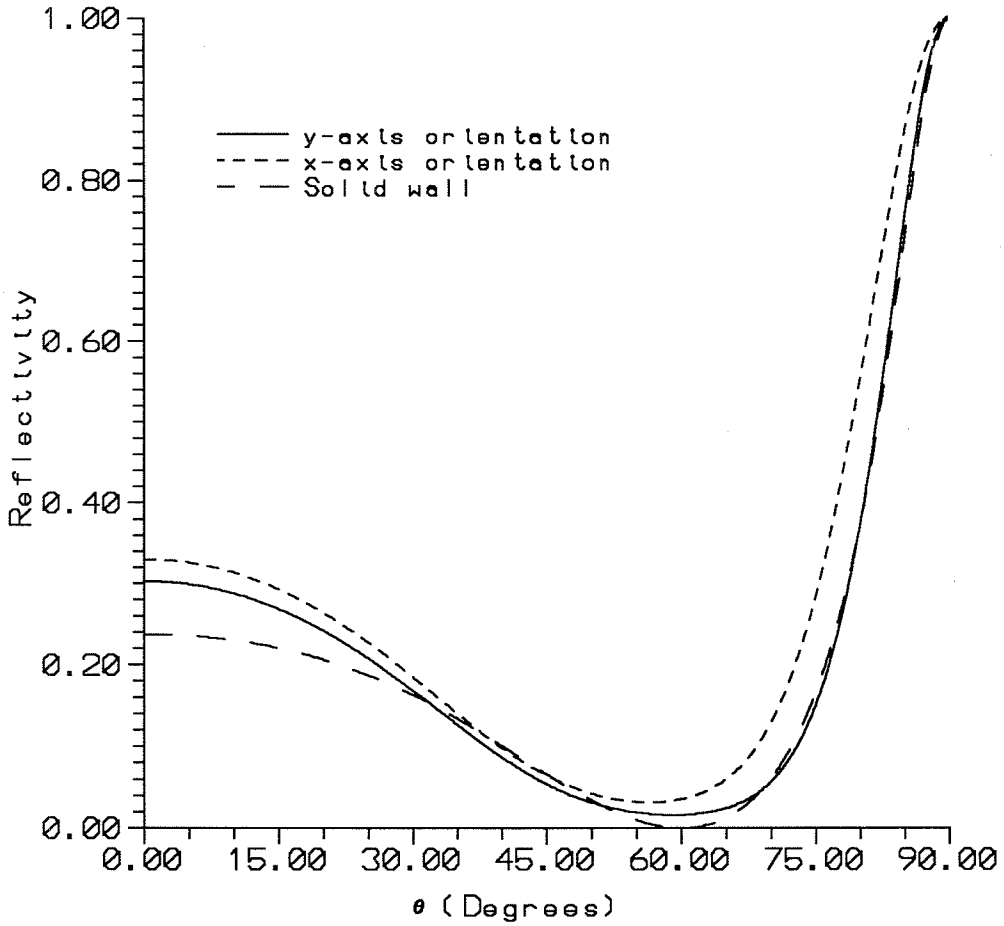

Figure 10. Reflectivity versus angle of incidence for a parallel polarized wave. These results are for block # 1 (see Table 1) with slabs oriented along both the $y-axis$ and $x-axis$ and with $f = 900$ MHz. The large dashed curve represents the results for a single layer slab of thickness equal to $2l_2 + l_3$, the solid curve represents the actual concrete block wall with the slabs oriented along the $y-axis$, and the small dashed curve represents the results for the actual concrete block wall with the slabs oriented along the $x-axis$.

Assume that a transmitting and receiving antenna are located 1 m from a wall. The power received (P_w) due to the wall reflection only, is given by:

$$P_w = 20 \log_{10} \left[\left| \frac{\Gamma}{x} e^{j(k x - \phi_\Gamma)} \right| \right] + P_o \quad [dB] \tag{19}$$

where P_o (in dB) is the transmitted power, k is the wavenumber; Γ and ϕ_Γ are the magnitude and phase of the reflection coefficient from the wall, respectively; and x is the total distance that the wave travels and is given by:

$$x = 2 \sqrt{w^2 + \left(\frac{d}{2}\right)^2} \tag{20}$$

where w is the distance between the wall and the transmitting and receiving antenna and d is the distance between the two antennas.

Figure 11 shows results for the received power as a function of antenna separation for a frequency of 900 MHz and for both antennas placed 1 m from the wall. The four plots in this figure correspond to a solid wall, a block wall oriented along the y-axis, a block wall oriented along the x-axis, and a perfect conductor. All these results were calculated assuming a perpendicularly polarized wave. These results indicate that for a long path length ($d > 500$ m) there is little difference between a solid wall, a composite wall, or a perfectly conducting wall. However, for short path lengths the power received by the solid wall or a perfectly conducting wall cannot reproduce the resonance behavior that is present in the composite walls. This figure illustrates that for short propagation paths, 10- to 20-dB inaccuracies can occur if one assumes the composite wall is treated as a solid wall.

As one might expect, the further the distance between the wall and the two antennas, the larger the separation distance between the antennas must be before the three curves coincide. Figure 12 illustrates results of the received power versus distance for a frequency of 900 MHz and for both antennas placed 4 m from the wall. For this example, the four curves correlate for $d > 1$ km.

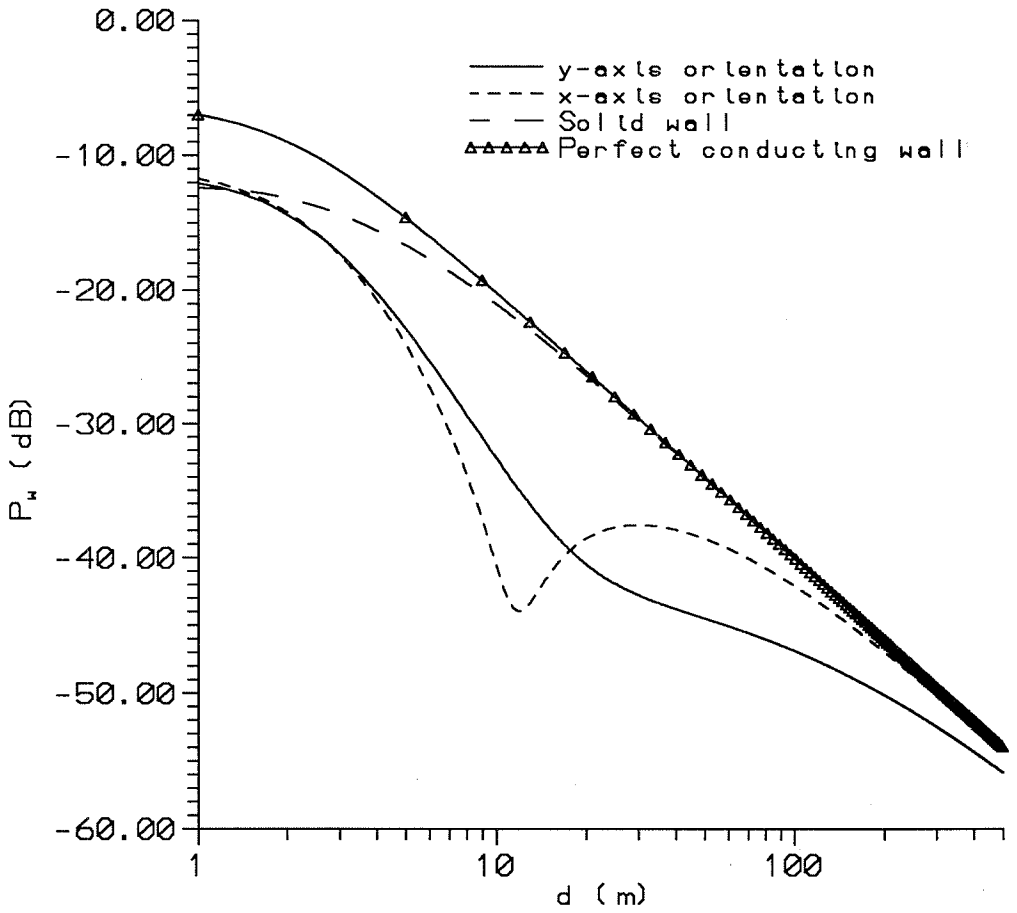

Figure 11. Reflected power off the wall versus antenna separation. These results are for block # 1 (see Table 1) with slabs oriented along the $y-axis$ and $f = 900$ MHz. The antennas are 1 m away from the wall.

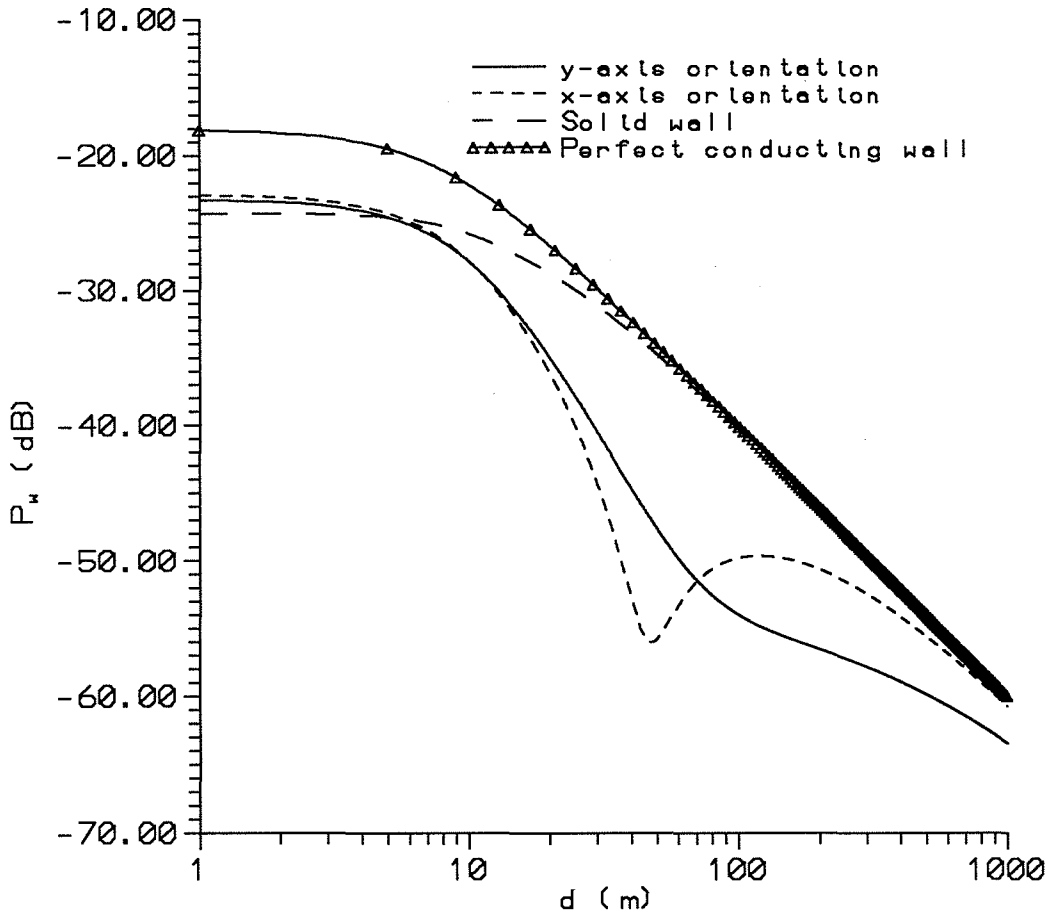

Figure 12. Reflected power off the wall versus antenna separation. These results are for block # 1 (see Table 1) with slabs oriented along the $y-axis$ and $f = 900$ MHz. The antennas are 4 m away from the wall.

In Figure 13 we show results for the total received power as a function of antenna spacing for an antenna placed above a perfectly conducting ground and between two walls. The results in Figure 13 are for a transmitter and receiver antenna spaced 1 m off of the ground and 1 m out from each wall. These two walls are assumed to be either a perfectly conducting wall, a single layer slab wall, or a concrete block wall. The received power is calculated by assuming that the total power is comprised of four different rays (Figure 3): the direct path, the ground reflection, and one reflection off each of the two walls. The predicted signal level is given by the following:

$$P_T = 20 \log_{10} \left[\left| \frac{e^{j k d}}{d} + \Gamma_G \frac{e^{j k s}}{s} + 2 \Gamma_w \frac{e^{j(k r - \phi_w)}}{r} \right| \right] + P_o \quad [dB] \tag{21}$$

where Γ_G is the reflection coefficient of the ground and for horizontal polarization $\Gamma_G = -1$ and for vertical polarization $\Gamma_G = 1$, Γ_w and ϕ_w are the magnitude and phase of the reflection coefficient of the walls; s (the reflection path off the ground) and r (the reflection path off the walls) are given by:

$$s = 2\sqrt{h^2 + \tfrac{d^2}{4}} \quad \text{and} \quad r = 2\sqrt{w^2 + \tfrac{d^2}{4}} \tag{22}$$

where h is the distance the antennas are above the ground, w is the distance the antennas are from the walls, and d is the separation of the two antennas.

The results are consistent with those shown in Figure 11. For small distance ($d < 1$ km) the results for the composite wall show a difference in received signal of 8 to 10 dB from the results for the other two types of walls. Figure 14 shows results for a transmitter and receiver antenna spaced 4 m away from each wall. This figure shows that between 40 and 500 m, the results for the block wall indicate an average of about 8- to 10-dB difference in received signal than that obtained from the solid or perfectly conducting wall. The nulls for the block wall are not as deep as those for the other two walls.

Depending upon frequency, the bulk material properties of the blocks, or the dimensions of the blocks, the composite wall may or may not behave like either a single slab wall or a

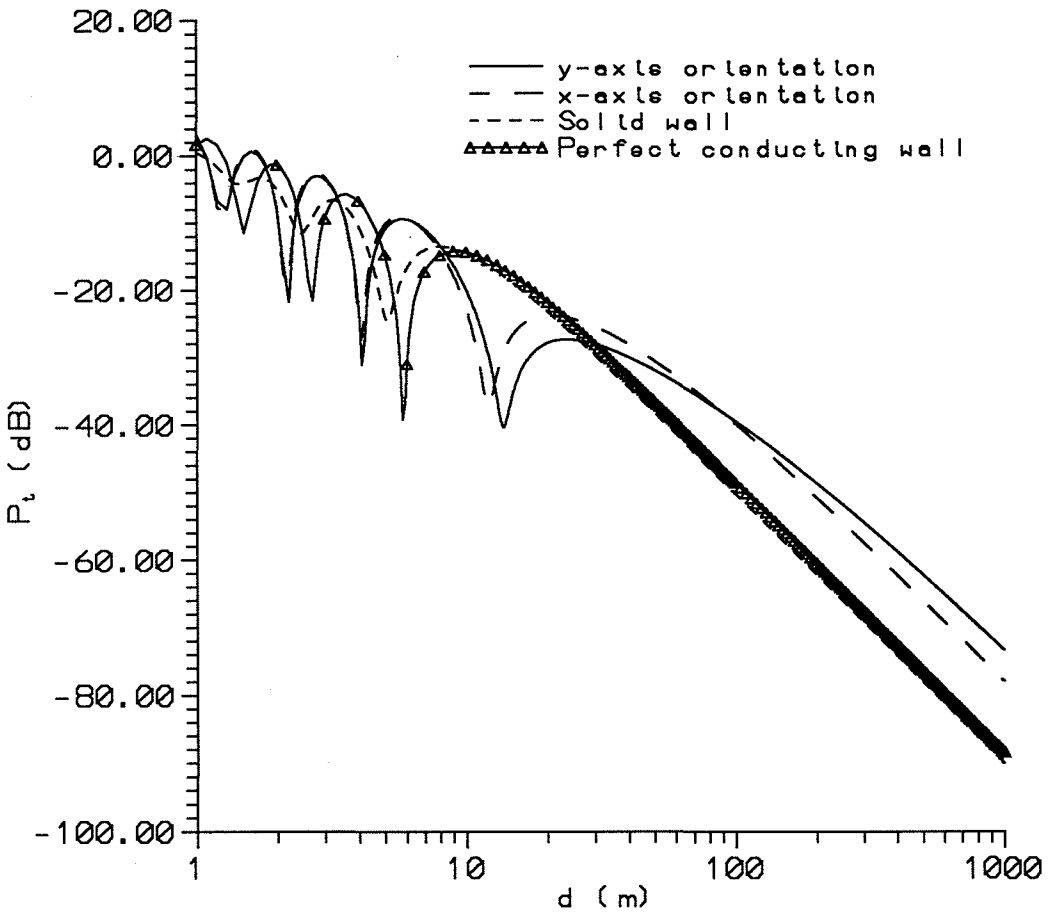

Figure 13. Received power versus antenna separation for the four-ray model. These results are for block # 1 (see Table 1) with slabs oriented along the $y-axis$ and $f = 900$ MHz. The antennas are 1 m off the ground and are spaced 1 m from each of the two walls.

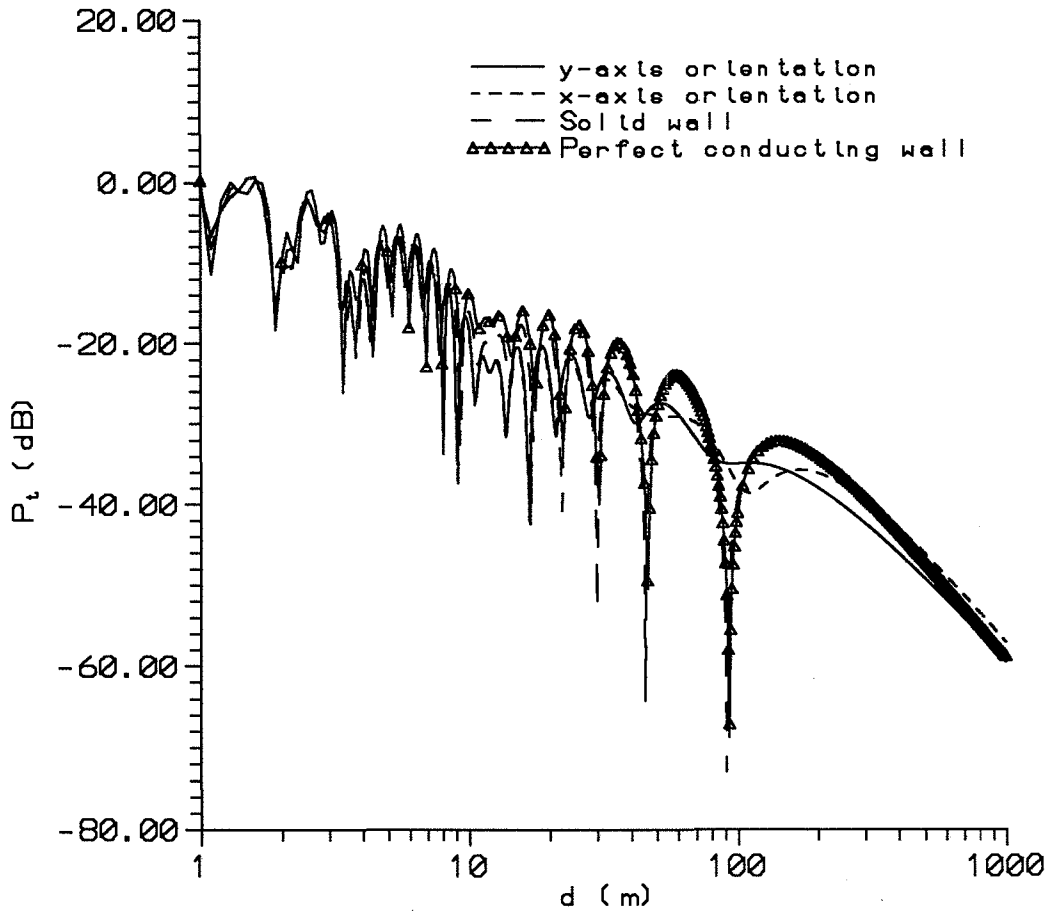

Figure 14. Received power versus antenna separation for the four-ray model. These results are for block # 1 (see Table 1) with slabs oriented along the $y-axis$ and $f = 900$ MHz. The antennas are 1 m off the ground and are spaced 4 m from each of the two walls.

perfectly conducting wall. Figures 15 and 16 show the results of the reflectivity for a wall composed of block # 2 (see Table 1). This block is identical to block # 1 with the exception that the dielectric constant (ϵ_r) is different. Figure 15 shows that for the perpendicular polarization (E-polarization), the block wall has very large values for the reflectivity for small incident angles, whereas the results for the solid slab have small values for the reflectivity for these small angles. For the perpendicular polarization, we should expect that if the total power received from the four-ray model (equation (21)) was calculated, then the results for the block wall would correlate fairly well with the perfectly conducting walls.

Figure 16 shows that for the parallel polarization (H-polarization) the reflectivity for block # 2 exhibits deep nulls, and further more, the results for the y-axis orientation composite wall corresponds very closely for large incident angles to the results for the solid wall. Therefore, the total predicted power from the composite wall is expected to correlate more closely to the solid wall than to the perfectly conducting wall. This is the case, and the results for the total received power for the four-ray model are shown in Figure 17. For an antenna separation between 5 and 60 meters, the signal predicted for a block wall is about 5 dB to 10 dB less than for a perfectly conducting wall.

Figures 18 and 19 show the reflectivity for a 7.2-cm (4-in) and 19.6-cm (8-in) block wall, respectively. The 7.2-cm (4-in) block wall corresponds to block # 3 in Table 1, and the 19.6-cm (8-in) block wall corresponds to block # 4 in Table 1. The results shown in these figures are for a perpendicular polarized wave. Results for the predicted signal levels of the four-ray model for these two block walls are shown in Figure 20 and 21.

The results in Figure 18 indicate that the reflectively of the composite wall is very similar to the results for the solid wall. Figure 20 shows that for the 7.2-cm (4-in) block wall, the predicted signal level correlates more closely with the solid wall than to the perfectly conducting wall. However, from Figure 20 it is shown that the total received power for the

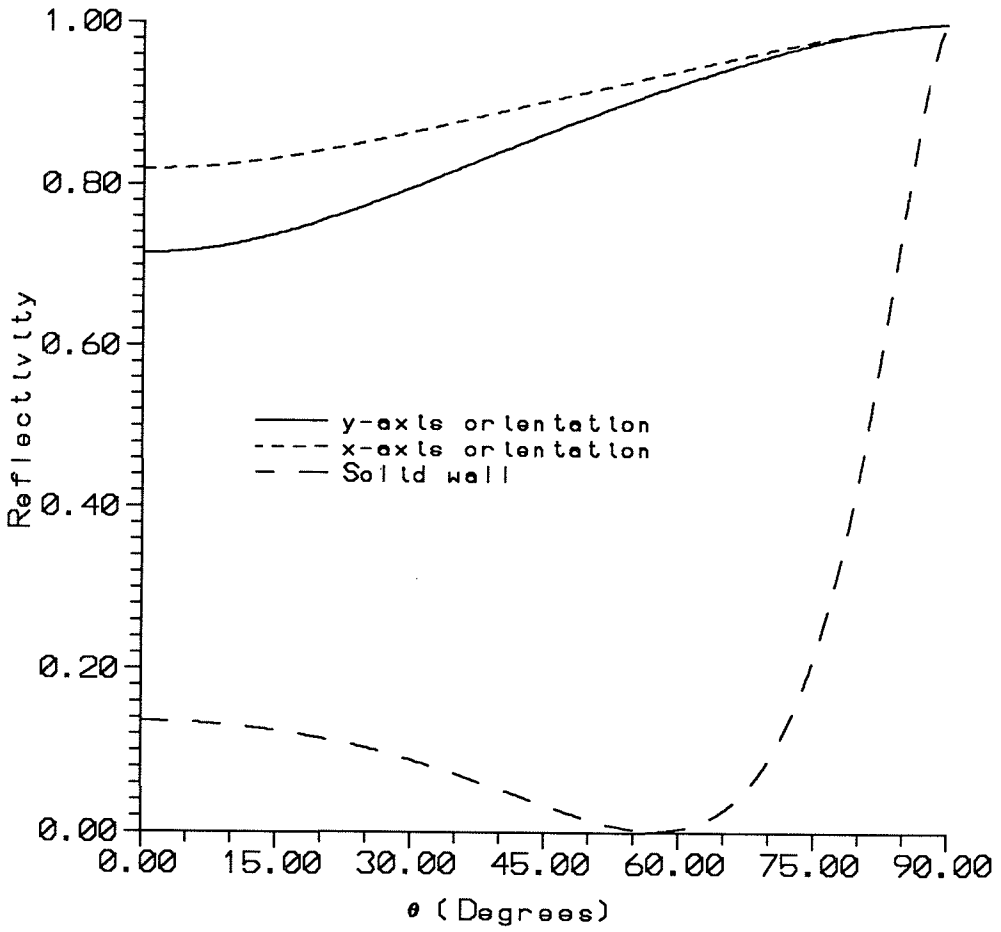

Figure 15. Reflectivity versus angle of incidence for a perpendicular polarized wave. These results are for block # 2 (see Table 1) with slabs oriented along both the $y-axis$ and $x-axis$ and with $f = 900$ MHz. The large dashed curve represent the results for a single layered slab of thickness equal to $2l_2 + l_3$, the solid curve represents the actual concrete block wall with the slabs oriented along the $y - axis$, and the small dashed curve represents the results for the actual concrete block wall with the slabs oriented along the $x - axis$.

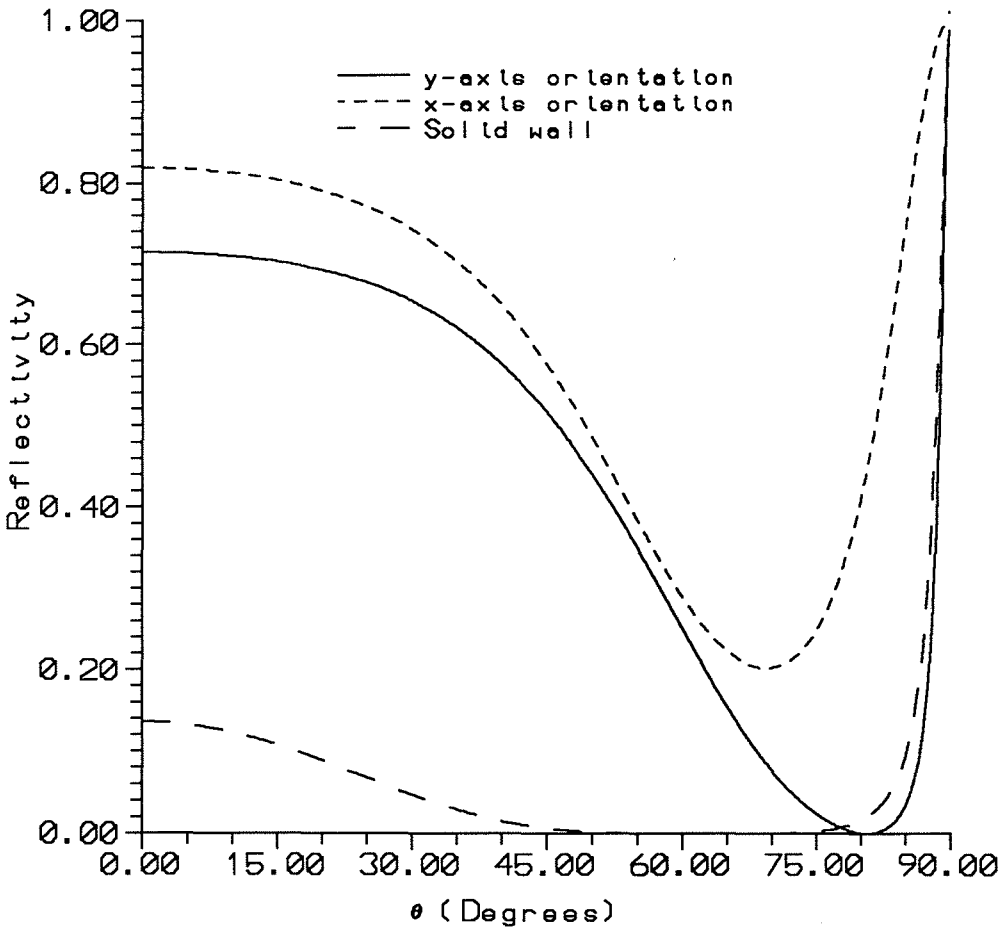

Figure 16. Reflectivity versus angle of incidence for a parallel polarized wave. These results are for block # 2 (see Table 1) with slabs oriented along both the $y - axis$ and $x - axis$ and with $f = 900$ MHz. The large dashed curve represent the results for a single layered slab of thickness equal to $2l_2 + l_3$, the solid curve represents the actual concrete block wall with the slabs oriented along the $y - axis$, and the small dashed curve represents the results for the actual concrete block wall with the slabs oriented along the $x - axis$.

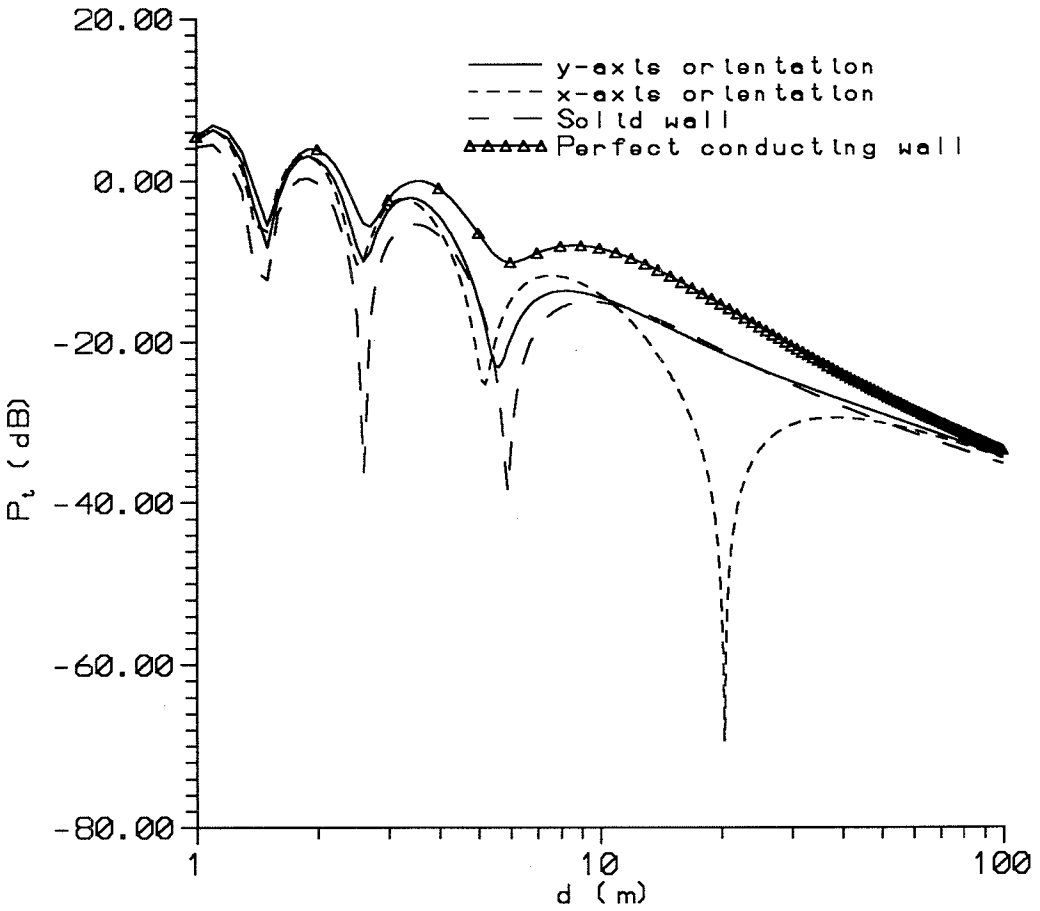

Figure 17. Received power versus antenna separation for the four-ray model. These results are for the parallel polarization for block # 2 (see Table 1) with slabs oriented along the $y - axis$ and $f = 900$ MHz. The antennas are 1 m off the ground and are spaced 1 m from each of the two walls.

solid and composite wall are not as close as might be expected upon examining the results in Figure 18, especially between 2 and 20 m. The total received power is a function of both the magnitude and phase of the reflection coefficient (Γ). The results in Figure 18 only depict the magnitude of Γ, the phase of Γ for the composite and solid walls can behave quit differently from each other depending upon the geometry and material properties of the walls, and this characteristic is equally important in determining the total received power.

These examples illustrate how the predicted signal level can vary for block walls with different geometries and material properties. Depending on the block wall parameters, the predicted signal level for short path propagation can correlate to either a solid slab wall, or to a wall composed of a perfect conductor. It can also behave differently from either of these two types of walls.

5. REFLECTION FROM A TWO-DIMENSIONAL BLOCK WALL

The two-dimensional composite structure shown in Figure 2 is replaced by the four-layer medium shown in Figure 5. Layers 1 and 4 are free space, layer 3 is a solid medium with $\epsilon_r = 6.1$, $\sigma = 1.95 \cdot 10^{-3}$ and $l_3 = 4.75\ cm$, and layer 2 is a periodic medium with effective material properties given by equations (8) and (9). For this medium it is assumed that $\epsilon_r = 6.1$, $\sigma = 1.95 \cdot 10^{-3}$, $a = 2.7\ cm$, $d = 15.3\ cm$ and $l_2 = 12.8\ cm$

Figure 22 shows results for the reflectivity of this composite structure for both perpendicular and parallel polarizations. Also shown in this figure are the results of a solid wall 17.55-cm thick, where $\epsilon_r = 6.1$ and $\sigma = 1.95 \cdot 10^{-3}$. Notice that the resonance behavior of the solid wall for the perpendicular polarization is different than that for the composite structure.

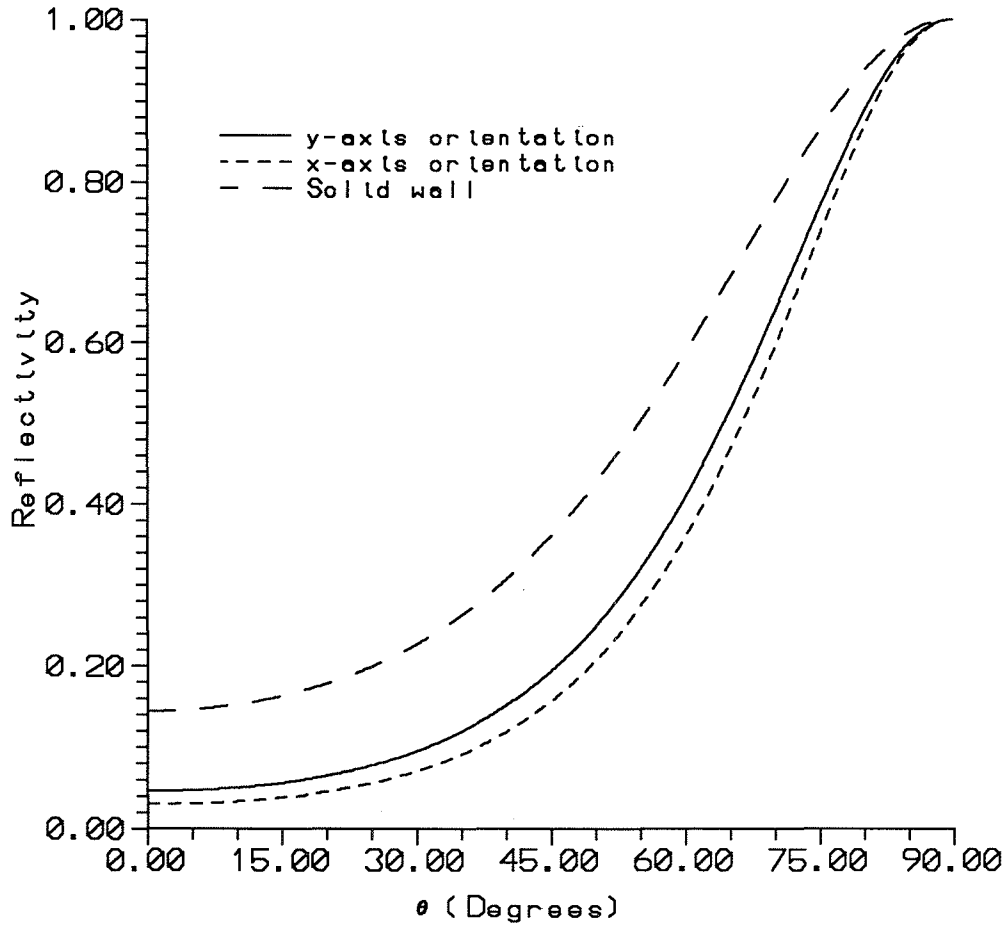

Figure 18. Reflectivity versus angle of incidence for a perpendicular polarized wave. These results are for a 7.2-cm concrete block wall (block # 3 in Table 1) with slabs oriented along both the $y-axis$ and $x-axis$ and with $f = 900$ MHz. The large dashed curve represents the results for a single layer slab of thickness equal to $2l_2 + l_3$, the solid curve represents the actual concrete block wall with the slabs oriented along the $y-axis$, and the small dashed curve represents the results for the actual concrete block wall with the slabs oriented along the $x-axis$.

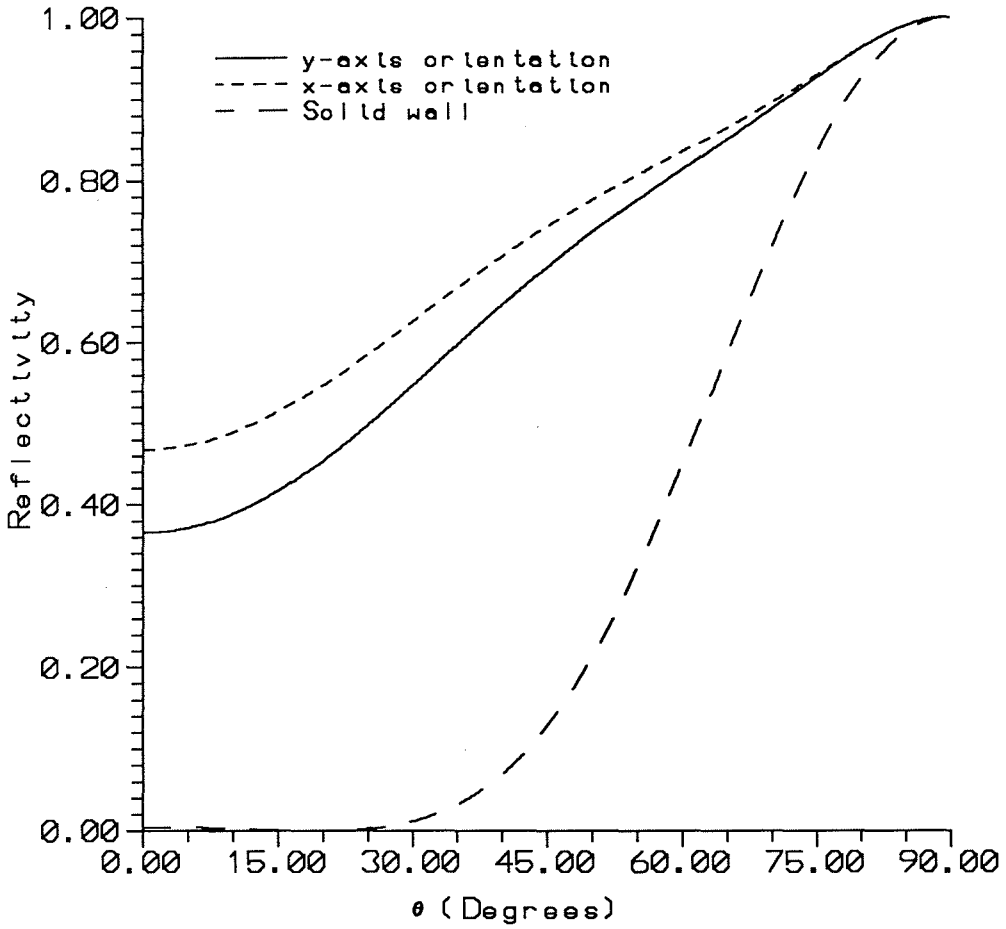

Figure 19. Reflectivity versus angle of incidence for a perpendicular polarized wave. These results are for an 19.6-cm concrete block wall (block # 4 in Table 1) with slabs oriented along both the $y-axis$ and $x-axis$ and with $f = 900$ MHz. The large dashed curve represents the results for a single layer slab of thickness equal to $2l_2 + l_3$, the solid curve represents the actual concrete block wall with the slabs oriented along the $y-axis$, and the small dashed curve represents the results for the actual concrete block wall with the slabs oriented along the $x-axis$.

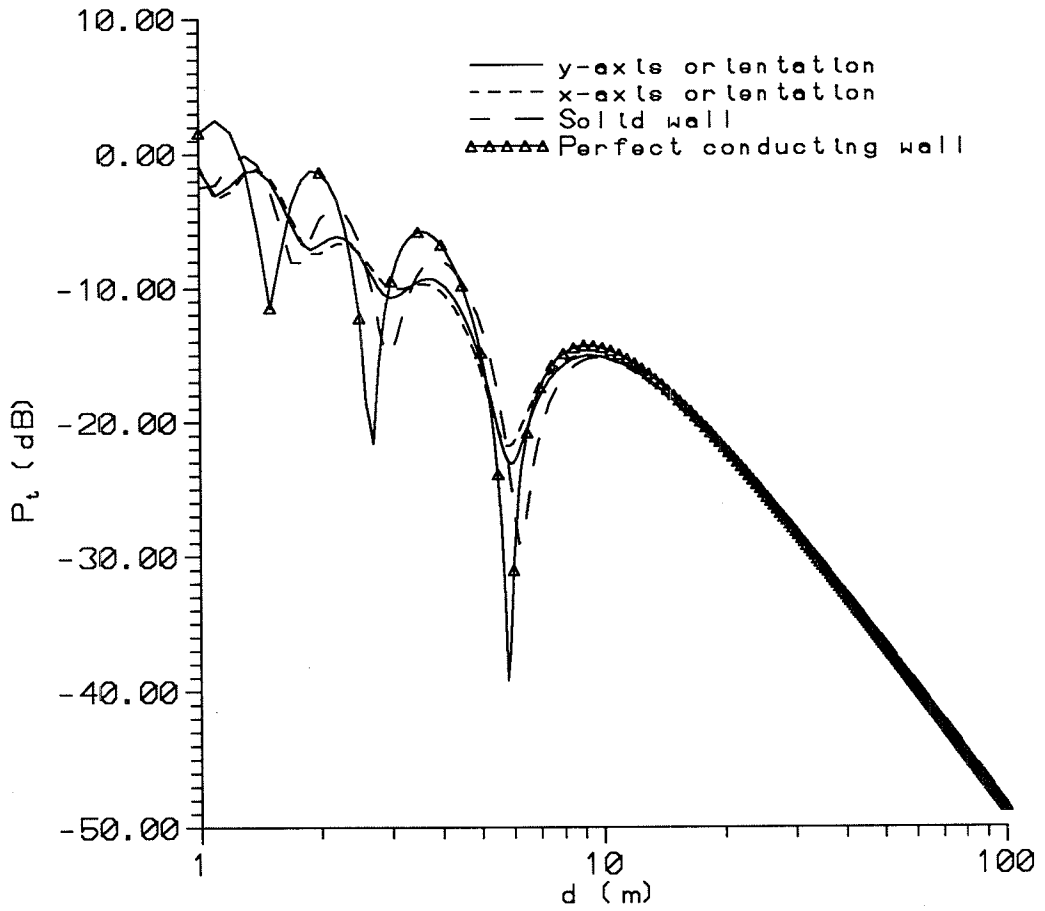

Figure 20. Received power versus antenna separation for the four-ray model. These results are for a 7.2-cm concrete block wall (block # 3) with slabs oriented along the $y-axis$ and $f = 900$ MHz. The antennas are 1 m off the ground and are spaced 1 m from each of the two walls.

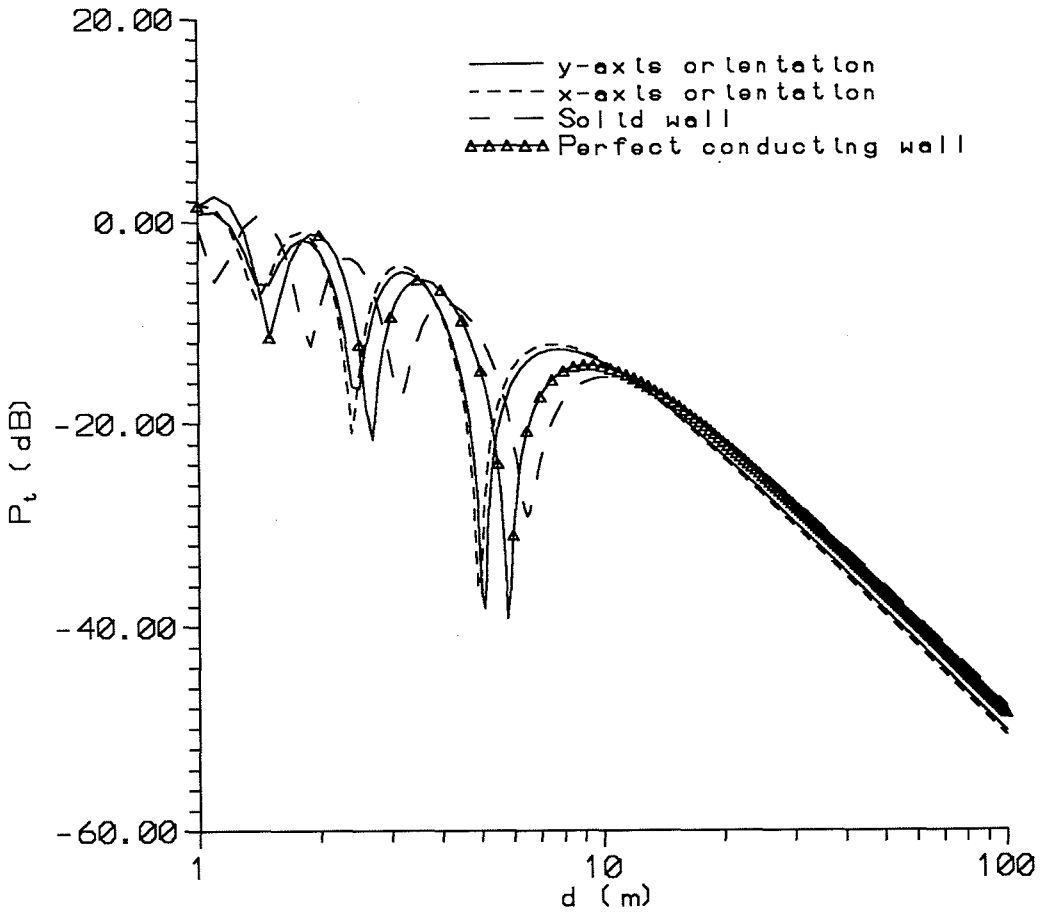

Figure 21. Received power versus antenna separation for the four-ray model. These results are for an 19.6-cm concrete block wall (block # 4) with slabs oriented along the $y-axis$ and $f = 900$ MHz. The antennas are 1 m off the ground and are spaced 1 m from each of the two walls.

Figure 23 illustrates the results of the received power for the four-ray model with a frequency of 900 MHz and the antenna placed 1 m from the wall. The results shown in this figure assume a solid wall, a composite two-dimensional structure, and a perfectly conducting wall. Here again, as for the concrete block wall, the results from the three different walls approach one another for long propagation paths. However, for short propagation paths (< 1 km) a difference of about 5 dB can be predicted. This again illustrates the importance of properly representing the wall reflections for short propagation paths.

6. VALIDITY OF THE EFFECTIVE MEDIUM MODEL

The underlining assumption in the effective material properties model used in this paper, is that the period of the structure is small compared to a wavelength. For how large of a period compared to a wavelength can we expect valid results? This question can be answered by referring to homogenization results for a similar problem.

In earlier work, one-dimensional wedges and two-dimensional pyramidal absorber structures were analyzed [33]-[35] using the same techniques presented here. Reference [34] and [35] illustrate that with the effective properties of the periodic absorbing structures, the reflection coefficients can be obtained by solving a classic inhomogeneous layered media problem. The theoretical reflection coefficient obtained with these effective material properties have been compared to both experimental results, [36] and [37], and to results obtained from a full numerical simulation of the absorbing materials, [34] and [38]. Experimental results from Ellam [36] and Pues [37] have indicated that the effective material properties model used to analyze the absorbing material were valid for a period as large as 1-3 free space wavelengths.

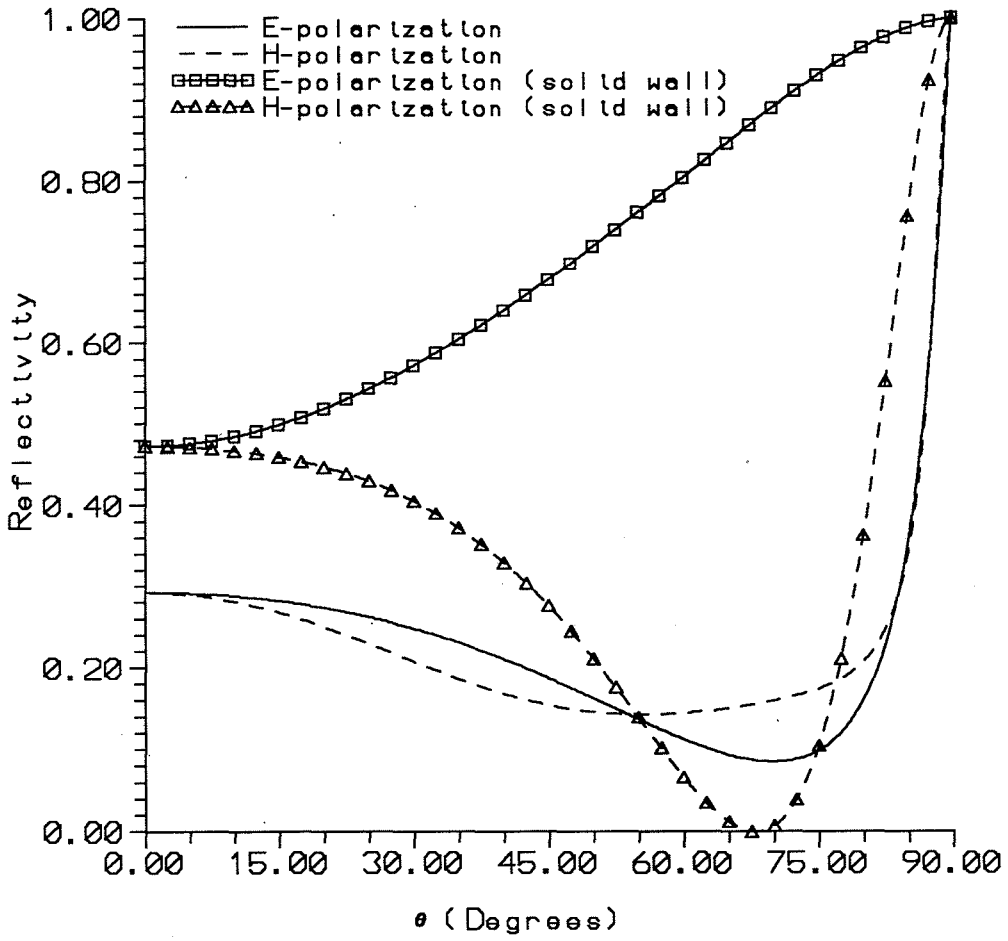

Figure 22. Reflectivity versus angle of incidence for a two-dimensional concrete block wall with $l_2 = 4.75$ cm, $l_3 = 12.8$ cm, $d = 15.3$ cm, $a = 2.7$ cm, $\epsilon_r = 6.05$, $\sigma = 1.95 \cdot 10^{-3}$, and with $f = 900$ GHz. The solid curve represents the results for the actual concrete block wall for the perpendicular polarization, the dashed curve represents the actual concrete block wall for the parallel polarization, the squares represent the the results for a single layer slab of thickness equal to $2l_2 + l_3$ for the perpendicular polarization, and the triangles represent the the results for a single layer slab of thickness equal to $2l_2 + l_3$ for the parallel polarization.

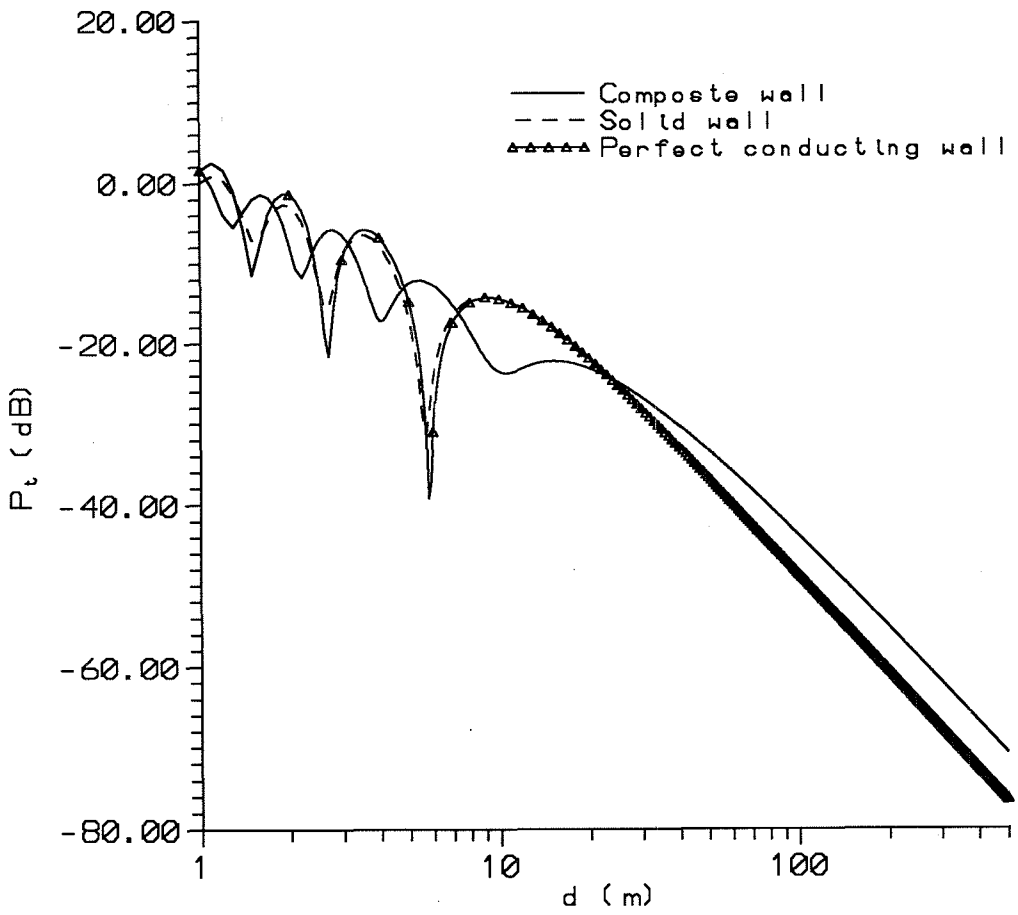

Figure 23. Received power for the four-ray model versus antenna separation. These results are for a two-dimensional block wall with $l_2 = 4.75$ cm, $l_3 = 12.8$ cm, $d = 15.3$ cm, $a = 2.7$ cm, $\epsilon_r = 6.05$, $\sigma = 1.95 \cdot 10^{-3}$, and with $f = 900$ MHz. The antennas are 1 m off the ground and are spaced 1 m from each of the two walls.

In [34] reflection coefficients calculated by using the effective material properties model were compared to results obtained from a moment-method calculation and excellent agreement was demonstrated. The results in this comparison were for a period of the structure equal to half a free space wavelength, and excellent agreement was demonstrated for incident angles as large as 90°. Using a finite difference time domain technique, Holloway, Mckenna, and DeLyser [38] have indicated that excellent agreement is achieved for a period as large as a free space wavelength for normal incidence. Agreement was also achieved for a period of 1/2 of a wavelength for incident angles as large as 90°.

These numerical and experimental results indicate that the effective material properties model presented here for the composite structure are accurate for periods at least as large as 1/2 to 1 free space wavelength and possibly even higher. The upper frequency limit for which the effective material properties of periodic structures can be used is currently being investigated [38].

The only results in the literature analyzing electromagnetic wave interaction with concrete block walls are those of Honcharenko and Bertoni [19]. We have made some comparison to their results, and for 900 MHz we get quantitatively similar, but not identical, results. Because of the error in Figure 4 of [19] we have to question if their other results are correct. Honcharenko and Bertoni [19] make no comparisons in their paper that suggest that their results are correct. We have compared our model to results from Bertoni's earlier paper [18] (the basis of [19]) and for a incident angle of 45°, agreement is achieved for a period of 1/2 wave length (λ).

Bertoni, Cheo, and Tamir [18] and Pinello, Lee, and Cangellaris [26] show that for a period greater than $\lambda/2$ for incident angles of 45°, higher order Floquet modes begin propagating. The homogenization model presented here cannot represent these higher order Floquet modes for large periods and the reflection coefficient based on homogenization would no longer be valid.

Watters [54] has investigated the problem of acoustical wave interactions with masonry block walls, but his results are not applicable here. Watters does however, suggest that some type of area weighted average model can be used to calculate transmission loss through these types of walls (see Figure 10 of [54]).

7. DISCUSSION AND CONCLUSION

We have presented a model for analyzing the reflections and transmissions of electromagnetic waves from periodic composite structures. With this model we have investigated the importance of correctly predicting electromagnetic field interaction with walls for short path propagation channels. For short path propagation (< 1 km), differences of 5-10 dB in received power can be predicted by modelling composite walls as either a single layer structure or as a perfectly conducting wall. This illustrates the importance of properly representing the wall reflections for short propagation paths.

For large propagation paths (> 1 km) the results for either the solid or the composite structures approach one another. This is expected because for large propagation paths, the angle of incidence of the wave on a wall approaches grazing (90°), thus regardless of the type of wall, the magnitude of the reflection coefficient approaches one. For long propagation paths, the magnitude of the reflected energy from the walls in the vicinity of the propagation path can be treated as if the walls behave as perfect conductors with little loss of generality. The one exception to this assumption, is for a periodic structure in which the period is large enough to guide energy in the structure. For this situation the periodic structure acts like a waveguiding structure, and energy can be carried away as waveguide modes, and so is not reflected off the surface in a spectral direction.

Some building materials consist of metal rods periodically spaced in concrete. One might first attempt to use the homogenization concepts discussed here to analyze such a problem. However, since there is a large material property contrast between the metal rods and the concrete, standard homogenization fails (see [55] and [38]) and the so-called *stiff* homogenization must be used. This approach has been used to tackle scattering from dense periodic space scatterers embedded in a dielectric [56], and details will be published later.

Even though the model presented for the reflection coefficient breaks down for large periods, the results still illustrate the importance for accurately predicting reflection for short distance propagation. Unfortunately once the period of the structure becomes large, simple expressions for the reflection coefficient are not available. Under these conditions one must resort to more complicated means, such as a Floquet type of analysis or a full numerical approach [12], [18], [19], [26], [27] and [57], to calculate the reflection coefficients.

8. REFERENCES

[1] H. L. Bertoni, W. Honcharenko, L. R. Maciel, and H. H. Xia, "UHF propagation prediction for wireless personal communications," *Proceeding of the IEEE*, vol. 82, no. 9, pp. 1333-1359, 1994.

[2] V. Erceg, S. Ghassemzadeh, M. Taylor, D. Li, and D. L. Schilling, "Urban/suburban out-of-sight propagation modeling," *IEEE Communication Magazine,* pp. 56-61, June, 1992.

[3] T. S. Yim and T. H. Siang, "A new propagation model for a street scene for micro-cellular communications," *in Proc. 1992 Int. Symp. on Electromagnetic Compatibility,* (Singapore, 7-9, Dec. 1992), pp. 200-207.

[4] R. A. Valenuela, "A ray tracing approach to predicting indoor wireless transmission," *in Proc. IEEE 43rd IEEE Vehicular Technology, Conf.* (Secaucus, N.J., 18-20, May 1993), pp. 214-218.

[5] Y. Yamaguchi, T. Abe and T. Sekiguchi, "Radio propagation characteristics in underground streets crowded with pedestrians," *IEEE Trans. Electromagn. Compat.,* vol. 30, no. 2, pp. 130-136, 1988.

[6] C. Bergljung and L. G. Olsson, "Rigorous diffraction theory applied to street microcell propagation," *in Proc. 1991 IEEE Global Telecommunication Conference,* (Phoenix, Az, 2-5, Dec. 1991), pp. 1292-1296.

[7] T. Takeuchi, M. Sako, and S. Yoshida, "Multipath delay prediction on a workstation for urban mobile radio environment," *in Proc. 1991 IEEE Global Telecommunication Conference,* (Phoenix, Az, 2-5, Dec. 1991), pp. 308-1312.

[8] A. J. Rustako, N. Amitay, G. J. Owens, and R. S. Roman, "Radio propagation at microwave frequencies for line-of-sight microcellular mobile and personal communications," *IEEE Trans. Veh. Technol.,* vol. 40, no. 1, pp. 203-210, 1991.

[9] E. Violette, R. Espeland, and K. C. Allen, "Millimeter-wave propagation characteristics and channel performance for urban-suburban environments," NTIA Report 88-239, Dec. 1988.

[10] K. C. Allen, "A model of millimeter-wave propagation for personal communication networks in urban settings," NTIA Report 91-275, April 1991.

[11] S. L. Chuang and J. A. Kong, "Scattering of waves from periodic surfaces," *Proceedings of the IEEE,* vol. 69, no. 9, pp. 1132-1144, 1981.

[12] B. Y. Myakishev, "Investigation of the reflection properties of a corrugated surface, for a plane wave at oblique incidence," (in Russian), *Trudy Moskovsk. Aviats. Institut.,* no. 98, pp. 5-30, 1958.

[13] L. N. Deriugin, "The reflection of a plane transverse-polarized wave from a rectangular comb," *Radiotekhnika,* vol. 15, no. 2, pp. 15-26, 1960.

[14] L. N. Deriugin, "The reflection of a longitudinally polarized wave from a rectangular comb," *Radiotekhnika,* vol. 15, no. 5, pp. 9-16, 1960.

[15] P. Beckmann and A. Spizzichino, *The Scattering of Electromagnetic Waves from Rough Surfaces.* New York: The Macmillan Company, 1963, ch. 4.

[16] J. A. Kong, *Electromagnetic Wave Theory.* New York: John Wiley & Sons, 1986, ch. 6.

[17] S. M. Rytov, "Electromagnetic properties of a finely stratified medium," *Soviet Physics JETP*, vol. 2, no. 3, pp. 466-475, May 1956.

[18] H. L. Bertoni and L. H. S. Cheo, and T. Tamir, "Frequency-selective reflection and transmission by a periodic dielectric layer," *IEEE Trans. Antennas Propagat.,* vol. 37, no. 1, pp. 78-82, 1989.

[19] W. Honcharenko and H. L. Bertoni, "Transmission and reflection characteristics at concrete block walls in the UHF bands proposed for future PCS," *IEEE Trans. Antenna Propagat.,* vol. 42, no. 2, pp. 232-239, 1994.

[20] A. Boag, Y. Leviation, and A. Boag, "Analysis of two-dimensional electromagnetics scattering from nonplanar periodic surfaces using a strip current model," *IEEE Trans. Antennas Propagat.,* vol. 37, no. 11, pp. 1437-1446, 1989.

[21] S. D. Gedney and R. Mittra, "Analysis of the electromagnetic scattering by thick grating using a combined FEM/MM solution," *IEEE Trans. Antennas Propagat.,* vol. 39, no. 11, pp. 1605-1614, 1991.

[22] K. Sarabandi and F. T. Ulaby, "High frequency scattering from corrugated stratified cylinders," *IEEE Trans. Antennas Propagat.,* vol. 39, no. 4, pp. 512-520, 1991.

[23] E. M. Inspektorov, "Calculation of the reflection from the surface of radio absorbing material", [Russian], *Izv. VUZ Radioelektronika,* vol. 27, no. 11, pp. 103-105, 1982.

[24] E. M. Inspektorov, *Chislennyi Analiz Elektromagnitnogo Vozbuzhdeniya Provodyashchikh Tel.* Minsk: Izdat. Universitetskoe, 1987, pp. 78-82.

[25] C. Cheon and V. V. Liepa, "Full wave analysis of infinitely periodic lossy wedges," *in Proc. 1990 IEEE Antennas and Propagation Symposium,* (Dallas, Tx, 7-11, May 1990), pp. 618-621.

[26] W. P. Pinello, R. Lee, and A. C. Cangellaris, "Finite Element Modeling of Electromagnetic Wave Interaction with Periodic Dielectric Structures," *IEEE Trans. Microwave Theory Tech.,* vol. 42, no. 12, pp. 2294-2301, 1994.

[27] R. Janaswamy, "Oblique scattering from lossy periodic surfaces with application to anechoic chamber absorbers," *IEEE Trans. Antennas Propagat.*, vol. 40, no. 2, pp. 162-169, 1992.

[28] E. Sanchez-Palencia, *Non-Homogeneous Media and Vibration Theory* (Lecture Notes in Physics no. 127). Berlin: Springer-Verlag, 1980, pp. 68-77.

[29] M. Codegone, "On the acoustic impedance condition for ondulated boundary," *Ann. Inst. Henri Poincaré Sect. A: Phys. Théorique*, vol. 36, pp. 1-18, 1982.

[30] G. Nguetseng, "Problèmes d'écrans perforés pour l'équation de laplace," M^2AN *Modélis. Math. Anal. Numér.*, vol. 19, pp. 33-63, 1985.

[31] R. R. DeLyser and E. F. Kuester, "Homogenization analysis of strip gratings," *J. of Electromagnetic Waves and Applications,* vol 5, no. 11, pp. 1217-1236, 1991.

[32] C. L. Holloway, "Edge and surface shape effects on conductor loss associated with planar circuits", Department of Electrical and Computer Engineering, University of Colorado at Boulder, CO, *MIMICAD Tech. Report No. 12,* April 1992.

[33] E. F. Kuester and C. L. Holloway, "A low-frequency model for wedge or pyramid absorber arrays - I: Theory," *IEEE Trans. Electromagn. Compat.*, vol. 36, no. 4, pp. 300-306, 1994.

[34] C. L. Holloway and E. F. Kuester, "A low-frequency model for wedge or pyramid absorber arrays - II: Computed and measured results," *IEEE Trans. Electromagn. Compat.*, vol. 38, no. 4, pp. 307-313, 1994.

[35] E. F. Kuester and C. L. Holloway, "Improved low-frequency performance of pyramid-cone absorbers for application in semi-anechoic chambers," *in Proc. 1989 IEEE National Symposium on Electromagnetic Compatibility*, (Denver, CO, 23-25, May 1989), pp. 394-399.

[36] T. Ellam, "Design and synthesis of compact absorber for EMC chamber applications," *in Proc. 1994 EMC/ESD International* , (Anaheim, CA, 12-15, April 1994), pp. 147-155.

[37] H. Pues, Personal communication, Dr. Pues is a research engineer with Emerson & Cuming Anechoic Chambers, Grace Electronic Materials, Westerlo, Belgium.

[38] C. L. Holloway, P. Mckenna, and R. DeLyser, "A numerical investigation on the accuracy of the use of homogenization for analyzing periodic absorbing arrays," *in Proc. 1995 International Symposium on Electromagnetic Theory, URSI*, (St. Petersburg, Russia, 23-26 May 1995), pp. 163-165.

[39] A. Bensoussan, J. Lions and G. Papanicolau, *Asymptotic Analysis for Periodic Structures.* Amsterdam: North-Holland, 1978.

[40] J. Lions, *Some Methods in the Mathematical Analysis of Systems and Their Control.* Beijing: Science Press, 1981, Chapter 1.

[41] N. S. Bakhvalov and G. P. Panasenko, *Homogenization: Averaging Processes in Periodic Media: Mathematical Problems in the Mechanics of Composite Materials.* Dordrecht: Kluwer Academic Publishers, 1989.

[42] E. Sanchez-Palencia, "Comportements local et macroscopique d'un type de milieux physiques hétérogènes," *Int. J. Eng. Sci.*, vol. 12, pp. 331-351, 1974.

[43] A. Potier, "Recherches sur l'intégration d'un systéme d'équations aux différentielles partielles á coefficients périodiques," *Comptes Rendus Assoc. Franç. Avancement Sci. (Bordeaux)*, session 1, pp. 255-272, 1872 [also in A. Potier, *Mémoires sur l'Électricité et l'Optique.* Paris: Gauthier-Villars, 1912, pp. 239-256].

[44] H. Chipart, "Sur la propagation de la lumière dans les milieux à structure périodique," *Comptes Rendus Acad. Sci. (Paris)*, vol. 178, pp. 319-321, 1924.

[45] J. B. Keller, "Effective behavior of heterogeneous media," *Statistical Mechanics and Statistical Methods in Theory and Application* (U. Landman, ed.). New York: Plenum Press, 1977, pp. 631-644.

[46] E. F. Kuester and C. L Holloway, "Comparison of approximations for effective parameters of artificial dielectrics," *IEEE Trans. Micr. Theory Tech.*, vol. 38, pp. 1752-1755, 1990.

[47] O. Wiener, "Lamellare Doppelbrechung," *Physikal. Zeits.*, vol. 5, pp. 332-338, 1904.

[48] H. G. Haddenhorst, "Durchgang von elektromagnetischen Wellen durch inhomogene Schichten," *Zeits. Angew. Physik*, vol. 7, pp. 487-496, 1955.

[49] R. Pottel, "Absorption elektromagnetischer Zentimeterwellen in künstlich anisotropen Medien," *Zeits. Angew. Physik*, vol. 10, pp. 8-16, 1958.

[50] L. M. Brekhovskikh, *Waves in Layered Media.* New York: Academic Press, 1960, pp. 79-86, 215-233.

[51] M. Nakamura and M. Hirasawa, "Bonds on effective conductivity of a composite by the finite element method," *J. Appl. Phys.,* vol. 54, pp. 4216-4217, 1983.

[52] Z. Hashin and S. Shtrikman, "A variational approach to the theory of the effective magnetic permeability of multiphase materials," *J. Appl. Phys.*, vol. 33, pp. 3125-3131, 1962.

[53] J. B. Keller, "A theorem on the conductivity of a composite medium," *J. Math. Phys.,* vol. 5, pp. 548-549, 1964.

[54] B. G. Watters, "Transmission loss of some masonry walls," *J. Acoustical Society of America,* vol. 31, no. 7, pp. 898-911, 1959.

[55] G. P. Panasenko, "Averaging of process in highly heterogeneous structures," *Sov. Phys. Dokl.,* vol. 32, no. 1, pp. 20-22, 1988.

[56] C. L. Holloway, "Reflections from an array of periodically spaced conducting scatterers," *In preparation for both a journal and a NTIA publication.*

[57] V. P. Malt'sev, " Scattering of plane wave by wedge-shaped absorbing periodic strucutre", *J. of Communications Technology and Electronics*, vol. 39, no. 12, pp. 139-144, 1994.

FORM NTIA-29
(4-80)

U.S. DEPARTMENT OF COMMERCE
NAT'L. TELECOMMUNICATIONS AND INFORMATION ADMINISTRATION

BIBLIOGRAPHIC DATA SHEET

	1. PUBLICATION NO.	2. Gov't Accession No.	3. Recipient's Accession No.
	96 - 326		

4. TITLE AND SUBTITLE

A Study of the Electromagnetic Properties of Concrete Block Walls for Short Path Propagation Modeling

5. Publication Date
October 1995

6. Performing Organization Code
NTIA/ITS

7. AUTHOR(S) Christopher L. Holloway, Patrick L. Perini, Ronald R. Delyser, and Kenneth C. Allen

9. Project/Task/Work Unit No.
5 910 5105

8. PERFORMING ORGANIZATION NAME AND ADDRESS

National Telecommunications & Information Administration
Institute for Telecommunication Sciences
325 Broadway
Boulder, CO 80303-3328

10. Contract/Grant No.

11. Sponsoring Organization Name and Address

same as above

12. Type of Report and Period Covered
NTIA

13.

14. SUPPLEMENTARY NOTES

15. ABSTRACT *(A 200-word or less factual summary of most significant information. If document includes a significant bibliography or literature survey, mention it here.)*

For short propagation paths, correctly representing reflectionsof electromagnetic energy from surfaces is critical for accurate signal level predictions. In this paper, the method of homogenization is used to determine the effective material properties of composite material commonly used in construction. The reflection and transmission coefficients for block walls and other types of materials calculated with these homogenized effective material properties are presented. The importance of accurately representing the reflections for signal level prediction models is also investigated. It is shown that a 5- to 10-dB error in received signal strength can occur if the composite walls are not handled appropriately. Such accurate predictions of signal propagation over short distance is applicable to microcellular personal communications services deployments in urban canyons as well as indoor wireless private branch exchanges and localarea networks.

16. Key Words *(Alphabetical order, separated by semicolons)*

Composite walls, concrete walls, effective material properties, homogenization, propagation modeling, reflection coefficient

17. AVAILABILITY STATEMENT

☐ UNLIMITED.

☐ FOR OFFICIAL DISTRIBUTION.

18. Security Class. *(This report)*
Unclassified

20. Number of pages
41

19. Security Class. *(This page)*
Unclassified

21. Price:

U.S. GOVERNMENT PRINTING OFFICE:1995-673-018/00137